DURAND, J., GRANIER, W., COT, L. & AVINENS, C. (1973). *C.R. Acad. Sci. Sér. C*, **277**, 101–103.
DURAND, J., GRANIER, W., COT, L. & GALIGNÉ, J. L. (1975). *Acta Cryst.* B**31**, 1533–1535.
GALIGNÉ, J. L., DURAND, J. & COT, L. (1974). *Acta Cryst.* B**30**, 697–701.
GERMAIN, G., MAIN, P. & WOOLFSON, M. M. (1970). *Acta Cryst.* B**26**, 274–285.
HAHN, T., LOHRE, G. & CHUNG, S. (1969). *Naturwissenschaften*, **56**(9), 459.
VILMINOT, S., COT, L. & MAURIN, M. (1976). *Rev. Chim. Minér.* **13**, 157–161.

Acta Cryst. (1978). B**34**, 391–403

The Crystal Structure of Low Tridymite

BY JOHN H. KONNERT

Laboratory for the Structure of Matter, Naval Research Laboratory, Washington, DC 20375, *USA*

AND DANIEL E. APPLEMAN

Department of Mineral Sciences, National Museum of Natural History, Smithsonian Institution, Washington, DC 20560, *USA*

(*Received* 25 *July* 1977; *accepted* 7 *September* 1977)

Low tridymite (SiO_2) from Plumas County, California, is triclinic, $F\bar{1}$, $a = 9{\cdot}932$ (5), $b = 17{\cdot}216$ (6), $c = 81{\cdot}864$ (9) Å, $\alpha = \beta = \gamma = 90°$; $Z = 320$ [SiO_2]. The structure was solved by a restrained-parameter structure-factor least-squares refinement procedure with a twinned crystal of orthorhombic diffraction aspect. The final conventional unweighted R value for 3170 reflections is 0·064. The structure can be described in terms of ten crystallographically distinct layers made up of oval rings of six linked tetrahedra. Average Si–O distances for each of the 80 tetrahedra range from 1·602 to 1·611 Å; Si–O–Si angles average 148·3° and range from 139·7 to 173·2°. There is no evidence for ordering of impurities. The structure is distinctly different from that of monoclinic low tridymite in which only one-third of the rings are oval and two-thirds are ditrigonal. Our data suggest that terrestrial low tridymite may be a lower-temperature form.

Introduction

Low tridymite, a polymorph of SiO_2, was originally found in andesitic volcanic rocks from the Cerro San Cristóbal, Mexico (vom Rath, 1868). Recently Gardner & Appleman (1974) have shown that these crystals, as well as tridymites from many other natural terrestrial occurrences, have the orthorhombic diffraction aspect F^{***} with approximate cell dimensions $a = 9{\cdot}9$, $b = 17{\cdot}1$, $c = 81{\cdot}6$ Å and compositions close to 98·5 at.% SiO_2. This cell differs significantly from that of monoclinic 'low tridymites' from meteorites and synthetic preparations (Dollase, 1967) and lunar rocks (Appleman, Nissen, Stewart, Clark, Dowty & Huebner, 1971; Dollase, Cliff & Wetherill, 1971) which have approximate dimensions $a = 18{\cdot}5$, $b = 5{\cdot}0$, $c = 23{\cdot}8$ Å, $\beta = 105{\cdot}7°$, space group Cc (Dollase, 1967). The structure of the monoclinic form has recently been reported (Dollase & Baur, 1976; Kato & Nukui, 1976).

The structure of a terrestrial low tridymite from Plumas County, California, is described in this paper. This investigation was originally begun because the suggested similarities between the framework topologies of tridymite and silica glass (Konnert & Karle, 1972) made a more precise knowledge of the tridymite structure desirable. A second goal of the work was to determine whether the small amounts of Al, K and Na usually present in tridymites played an essential role in stabilizing the structure. Thirdly, we wished to elucidate the structural differences between the terrestrial and meteoritic forms. A preliminary account of this study was presented to the 1975 Annual Meeting of the Mineralogical Society of America (Konnert & Appleman, 1975).

Experimental

The crystal selected for structure analysis in this study was obtained from a rhyolitic volcanic rock from Plumas County, California, in the Collections of the Smithsonian Institution, National Museum of Natural

History specimen No. 121899. Tridymite from this locality shows less twinning than most natural specimens. The particular crystal which we used showed no evidence of pseudo-hexagonal twinning on precession and Weissenberg X-ray diffraction photographs. Zero- and upper-level nets were compatible with diffraction aspect F^{***}, orthorhombic (Gardner & Appleman, 1974). All reflections registered as sharp spots, with only a little very weak diffuse streaking parallel to **c***.

Several crystals from the Plumas County specimen were analyzed with an ARL SEMQ electron microprobe, with standard techniques. Many points on each crystal were analyzed individually. The results show an average composition $(Si_{0.99}Al_{0.01}K_{0.002}Na_{0.003}Ti_{0.001})O_2$. There is no significant variation within crystals, or from crystal to crystal. Thus, the analyzed material is approximately 99 mol% SiO_2.

X-ray diffraction data were collected on a Picker FACS-I diffractometer with a 1° min^{-1} scan speed and 20 s counting time on each background, with Ni-filtered Cu $K\alpha$ radiation. Special collimators were fitted to reduce background. No deviations from orthorhombic symmetry and no evidence of split reflections were observed. Lattice parameters, determined by least-squares refinement of 2θ angles for selected single-crystal reflections measured on the FACS-I, are: a = 9·932 (5), b = 17·216 (6), c = 81·864 (9) Å for the orthorhombic F cell. 3170 diffraction maxima were collected to $2\theta = 126°$.

The X-ray diffraction intensity data were corrected for Lorentz and polarization effects. Absorption corrections were made with the programs of Stewart, Kruger, Ammon, Dickinson & Hall (1972), μ(Cu $K\alpha$) = 78·64 cm^{-1}. The volume of the irregular crystal fragment used in the study was 0·002 mm^3. A single isotropic extinction parameter (Zachariasen, 1967) was refined throughout the investigation.

Determination of the trial structure

Precession and Weissenberg photographs indicated the diffraction symmetry to be *Fmmm*. Such symmetry for a single crystal would limit the possible space groups to *F*222, *Fmm*2, or *Fmmm*. However, inspection of the *hk*0 Patterson map revealed that the projected electron densities for the 20 layers were approximately superimposed, were incompatible with the above space groups, and compatible with plane group *pg*. In fact, with exact overlap of the layers assumed, refinement (with isotropic B's) of the two Si atoms and the three O atoms of plane group *pg* resulted in a conventional unweighted R = 0·19. The impossibly high B values of 3–4 for the Si atoms and 5–6 for the O atoms indicated, not surprisingly, that the assumption of layer overlap is not strictly valid. The R of 0·19 did, however, strongly suggest that it would not be fruitful to proceed under the assumption that the space group was *F*222, *Fmm*2 or *Fmmm*.

All values of $|E| > 1·08$ (~1500) were associated with the reflections of parity *ggg*. Further, all values of $|E| > 2·14$ (~140) were associated with a diffraction pattern of symmetry *mmmP–n–* with a halving of the cell dimensions. Space group $P2_1nm$, with *hk*0 projection *pg*, is consistent with this diffraction pattern. A phase determination was carried out in space group $P2_1nm$ with the symbolic addition procedure (Karle & Karle, 1966), and a resulting E map indicated a possible framework of Si atoms. The initial trial structure was obtained by placing the O atoms midway between the bridged Si atoms.

Refinement of the structure

Refinement of the trial structure was carried out in several stages. As mentioned, all values of $|E| > 1·07$ were of parity *ggg*. The first stage of the refinement was carried out with the *ggg* data in space group $P2_1$ with the unique direction coinciding with the a axis of the orthorhombic cell. The *hk*0 projection of $P2_1$ has symmetry *pg*. A twin plane perpendicular to **c** was assumed such that $I_c(hkl) = I'_c(hkl) + I'_c(hk\bar{l})$. Several cycles of refinement reduced the R value from 0·40 to 0·22 for the *ggg* data. The R value for the *uuu* data was, of course, 1·00 with an overall R of ~0·40.

A probable cause for the orthorhombic diffraction was the presence of more than one type of twinning. In order to investigate such possibilities, each intensity was expressed as the sum of four calculated intensities:

$$I_c(hkl) = k_1 I'_c(hkl) + k_2 I'_c(hk\bar{l}) + k_3 I'_c(\bar{h}kl) + k_4 I'_c(\dot{h}k\bar{l}).$$

Intensities of the ith twin component were scaled with k_i. The refinement was then carried out in space group $F1$ with 240 atoms in the asymmetric unit. A point to note is that all four I_c components of each observation may refine to the same value if the true symmetry is orthorhombic. They may refine to pairs of equal values if the true symmetry is monoclinic, or they may, as turned out to be the case, all be different if the symmetry is triclinic. If the assumption of complete overlap (each observation being the sum of four intensities) were not correct, it should not be possible to attain a suitably low R value.

A restrained-parameter structure-factor least-squares refinement procedure was formulated at this stage. The technique is described elsewhere (Konnert, 1976) and will only be discussed briefly here. It combines the conditional structure-factor least-squares procedure described by Waser (1963) with the conjugate gradient (CG) method for solving linear systems (Hestenes & Stiefel, 1952). The sum of squared residuals to be

Table 1. *Final atomic positions for low tridymite*

All values are fractional coordinates of the F cell multiplied by 10^5. Si atoms are identified by a layer number (in parentheses) and an atom number (1–8); the atoms are numbered in the same way in each layer. O atoms within a layer are described in the same way as the Si atoms; O atoms shared between layers have both layer numbers in parentheses.

ATOM	X	Y	Z	ATOM	X	Y	Z	ATOM	X	Y	Z
SI(1)1	6049	3633	3414	O(1,2)1	2331	2880	5321	O(4) 5	-6677	13958	17288
SI(1)2	56126	3679	3371	O(1,2)2	53202	3557	5282	O(4) 6	53602	10036	17960
SI(1)3	-2022	19793	1846	O(1,2)3	18855	30450	4704	O(4) 7	-13692	28276	17792
SI(1)4	23025	28978	2831	O(1,2)4	68116	30149	4695	O(4) 8	11713	24625	18189
SI(1)5	48204	19712	1779	O(2,3)1	-6621	22910	9828	O(4) 9	36134	20851	17220
SI(1)6	72606	29128	2822	O(2,3)2	45120	22872	9819	O(4)10	60790	24769	18233
SI(1)7	31136	46063	1895	O(2,3)3	28736	43393	10126	O(4)11	29727	35425	17561
SI(1)8	81084	46158	1933	O(2,3)4	78692	42769	10194	O(4)12	67902	38824	17331
SI(2)1	1300	5235	7211	O(3,4)1	3987	6824	14807	O(5) 1	-4879	-1691	21988
SI(2)2	48576	3038	7135	O(3,4)2	53585	6510	14851	O(5) 2	20109	2038	22560
SI(2)3	-1645	22688	7960	O(3,4)3	19016	26991	15158	O(5) 3	45224	-2256	22162
SI(2)4	23070	31107	6598	O(3,4)4	69419	27038	15271	O(5) 4	70138	2185	22520
SI(2)5	46080	20317	7936	O(4,5)1	-6233	19435	20250	O(5) 5	1610	12601	22966
SI(2)6	71072	28419	6591	O(4,5)2	43292	18790	20259	O(5) 6	50938	12330	23024
SI(2)7	25859	46761	8318	O(4,5)3	27472	47082	19647	O(5) 7	-16976	23072	23071
SI(2)8	73949	44146	8340	O(4,5)4	79075	46998	19732	O(5) 8	7875	27201	22448
SI(3)1	5429	4645	12921	O(5,6)1	3607	890	24997	O(5) 9	32898	23136	23066
SI(3)2	55652	4513	12951	O(5,6)2	54753	924	25073	O(5)10	57759	26756	22387
SI(3)3	-2557	21178	11701	O(5,6)3	20233	32513	25050	O(5)11	26947	37294	22080
SI(3)4	22884	28380	13270	O(5,6)4	69557	32268	25029	O(5)12	76357	37077	22090
SI(3)5	48158	21099	11717	O(6,7)1	-6081	19694	29712	O(6) 1	-13495	-1919	27293
SI(3)6	72795	28732	13375	O(6,7)2	43250	19703	29745	O(6) 2	11728	1166	28050
SI(3)7	30672	45008	12047	O(6,7)3	28913	46581	30342	O(6) 3	36767	-2723	27257
SI(3)8	80469	45095	12077	O(6,7)4	78507	46136	30288	O(6) 4	61405	1162	28149
SI(4)1	-806	5747	16665	O(7,8)1	3549	7231	35209	O(6) 5	-4016	12214	26904
SI(4)2	51258	3123	16666	O(7,8)2	54098	6541	35093	O(6) 6	44879	11770	26981
SI(4)3	-3431	21530	18369	O(7,8)3	18331	26704	34864	O(6) 7	-23071	22311	27351
SI(4)4	24039	27072	17021	O(7,8)4	69788	26518	34786	O(6) 8	1841	26978	27030
SI(4)5	48592	18696	18403	O(8,9)1	-6560	22485	40227	O(6) 9	26732	22413	27369
SI(4)6	71198	29733	17140	O(8,9)2	44709	22556	40200	O(6)10	51778	26532	27027
SI(4)7	26630	44539	17770	O(8,9)3	28665	42878	39814	O(6)11	20067	36812	28124
SI(4)8	73858	47061	17894	O(8,9)4	79172	43183	39803	O(6)12	69288	36573	28107
SI(5)1	4792	3540	23125	O(10,9)1	2675	2229	44667	O(7) 1	-13170	-455	33348
SI(5)2	54997	3394	23180	O(10,9)2	53965	2918	44729	O(7) 2	11483	3043	32267
SI(5)3	-3233	20609	22157	O(10,9)3	19695	30664	45287	O(7) 3	36017	74	33242
SI(5)4	22078	30081	23164	O(10,9)4	68300	30920	45242	O(7) 4	61297	-3472	32792
SI(5)5	46402	20260	22158	O(10,1)1	-5068	17436	49912	O(7) 5	-6702	13839	32644
SI(5)6	71696	29734	23155	O(10,1)2	45126	17230	49990	O(7) 6	53016	10446	31991
SI(5)7	29700	46113	21579	O(10,1)3	28663	48885	50083	O(7) 7	-13852	28144	32215
SI(5)8	79829	45915	21663	O(10,1)4	78581	48869	50049	O(7) 8	11564	24608	31821
SI(6)1	-500	3156	26833	O(1) 1	-3453	-2233	2397	O(7) 9	35817	21043	32810
SI(6)2	49360	2861	26878	O(1) 2	21504	1065	3152	O(7)10	60566	25037	31821
SI(6)3	-7624	20251	27784	O(1) 3	46516	-2383	2440	O(7)11	29305	35586	32543
SI(6)4	17311	29695	26892	O(1) 4	71548	966	3108	O(7)12	68387	38747	32871
SI(6)5	42106	20037	27810	O(1) 5	3828	12458	2849	O(8) 1	-4270	-2487	37553
SI(6)6	67164	29420	26879	O(1) 6	54350	12344	2711	O(8) 2	20763	1843	37297
SI(6)7	24310	45700	28464	O(1) 7	-15552	22774	2709	O(8) 3	45804	-2593	37506
SI(6)8	74099	45386	28401	O(1) 8	9752	26258	1843	O(8) 4	70792	1982	37353
SI(7)1	-1127	5741	33366	O(1) 9	34720	22544	2695	O(8) 5	2510	12080	38207
SI(7)2	51099	3461	33274	O(1)10	59632	26374	1782	O(8) 6	52151	12008	38091
SI(7)3	-3549	21523	31602	O(1)11	28313	36924	2027	O(8) 7	-15424	22357	37223
SI(7)4	23592	27164	33012	O(1)12	77913	37097	2058	O(8) 8	9630	26815	37864
SI(7)5	48141	19216	31597	O(2) 1	-13521	3536	7910	O(8) 9	34475	22541	37221
SI(7)6	71254	29525	32940	O(2) 2	12074	451	8279	O(8)10	59553	26715	37730
SI(7)7	26507	44681	32239	O(2) 3	36614	-3305	7245	O(8)11	27131	37337	36860
SI(7)8	73711	46883	32151	O(2) 4	60971	404	8268	O(8)12	77472	37183	36876
SI(8)1	5402	4624	37071	O(2) 5	4317	14369	7451	O(9) 1	-13518	2894	42062
SI(8)2	55433	4489	37002	O(2) 6	42613	11183	7778	O(9) 2	12484	585	41725
SI(8)3	-2367	20997	38348	O(2) 7	-13907	25131	6786	O(9) 3	37026	-3506	42775
SI(8)4	22606	28414	36728	O(2) 8	10255	29035	7728	O(9) 4	61250	-547	41758
SI(8)5	47769	20929	38290	O(2) 9	35300	25204	6899	O(9) 5	3729	14034	42652
SI(8)6	72917	28317	36679	O(2)10	60949	21645	7209	O(9) 6	43439	10910	42224
SI(8)7	30406	44985	37919	O(2)11	27766	39862	7004	O(9) 7	-13450	25449	43264
SI(8)8	80457	44962	37903	O(2)12	68080	36035	7652	O(9) 8	10837	28407	42256
SI(9)1	1089	4822	42801	O(3) 1	-3956	-2582	12417	O(9) 9	35841	24435	43203
SI(9)2	49177	2779	42869	O(3) 2	20800	2253	12546	O(9)10	61450	21651	42794
SI(9)3	-1648	22402	42095	O(3) 3	45876	-2388	12378	O(9)11	28704	38952	42918
SI(9)4	23522	30330	43401	O(3) 4	71016	1902	12657	O(9)12	68536	35960	42246
SI(9)5	46602	20096	42080	O(3) 5	1672	12187	11855	O(10) 1	-11012	-2326	47172
SI(9)6	71384	28565	43382	O(3) 6	53102	12274	11909	O(10) 2	13973	2249	47529
SI(9)7	26175	45878	41648	O(3) 7	-15153	23020	12863	O(10) 3	38978	-2228	47128
SI(9)8	74321	44246	41648	O(3) 8	9963	26688	12146	O(10) 4	64061	2355	47609
SI(10)1	89	3822	46580	O(3) 9	34668	22426	12767	O(10) 5	-4298	12673	46855
SI(10)2	50365	3917	46628	O(3)10	59670	27066	12288	O(10) 6	45817	12756	46933
SI(10)3	-6794	19996	48037	O(3)11	27857	37158	13039	O(10) 7	-22182	22704	47767
SI(10)4	18252	29559	47201	O(3)12	77435	37635	13196	O(10) 8	2843	27144	47573
SI(10)5	43200	20000	48127	O(4) 1	-12477	-657	16729	O(10) 9	27839	22882	47931
SI(10)6	68040	29548	47172	O(4) 2	11944	3418	17769	O(10)10	52864	27213	47694
SI(10)7	25501	46482	48221	O(4) 3	36308	-436	16748	O(10)11	20922	37595	48142
SI(10)8	75445	46519	48184	O(4) 4	61930	-3701	17025	O(10)12	71419	37524	48105

minimized, θ, is a function not only of the observed and calculated intensities, but also of the ideal and calculated distances. The form of θ is:

$$\theta = \sum_i w_i(|F_o|_i - |F_c|_i)^2 + \sum_l w(d'^2_l - d^2_{c,l})^2$$

where i may range over all or just a portion of the intensity data, and l ranges over the distances to be restrained. An ideal distance is designated as d' and a calculated one as d_c. The weight assigned to an observation is w. Rapid, meaningful convergence may be obtained by calculating only those elements in the matrix of the normal equations that are related to the restraint equations. This corresponds to about 4% of one half of the symmetric matrix for the case of interest. The derivative matrix is not inverted and remains unaltered during solution of the normal equations by the CG method. Thus, the advantages of a sparse matrix are retained.

The number of structural parameters to be determined by the intensity data is greatly reduced by restraining the bond distances.

Correlations of the shifts, due to the make-up of the matrix, reduce the problem to one largely of torsions. Therefore, a much smaller intensity subset is required than would be the case without the restraints. Since calculation of the structure factors and their derivatives is the time-consuming step of a refinement cycle, employing a limited number of structure factors facilitates the evaluation of different models. The 320 Si–O distances were restrained to be near 1·61 Å, the 480 O–O distances of the tetrahedra to 2·63 Å and the 160 shortest Si–Si distances to 3·08 Å.

When atomic positions are only approximately known, it is advantageous to use a subset of intensity data consisting of a low-angle shell of data. The lower-angle data correspond to large interplanar spacings, and, therefore, the derivatives involved in the Taylor expansion on the structure factors are valid over a greater range of atomic coordinates. Of the 3170 diffraction data collected, the initial cycles were carried out with the ~600 data with $(\sin\theta/\lambda) < 0{\cdot}33$. The centroid of the molecule was constrained with three Lagrangian multipliers, *i.e.* the sum of the shifts of the x coordinates was constrained to zero as were the sums of the y and z shifts. Four thermal parameters were used to describe the system. All Si atoms were given the same isotropic B. A single anisotropic ellipsoid was used to describe the O atoms. The orientation of the ellipsoid for each O atom was fixed by the atomic environment of the atom. One axis was fixed parallel to the line connecting the bridged Si atoms, and one axis perpendicular to the Si–O–Si plane. With the inclusion of four scale factors, three Lagrangian multipliers, and one isotropic extinction parameter, 732 parameters were simultaneously varied on each cycle. After several cycles with $w_i = 1/75^2$ and $w = (6/d')^2$, the conventional R was 11% for the 600 data refined and 13% for all data. Subsequent cycles, with $w_i = (1/75)^2$, $w_l(\text{Si–O}) = (8{\cdot}4/d')^2$, $w_l(\text{O–O}) = (3{\cdot}1/d)^2$ and $w_l(\text{Si–Si}) = 1{\cdot}0$ reduced R to 8·9%.

A difference Fourier map was computed at this stage. Because of the twinning, this was not a conventional difference map. A decision had to be made as to how ΔI would be apportioned among the four intensities involved. From among the infinite number of ways of doing this, one was chosen where the differences for the four reflections were set equal:

$$I_o = \sum_{i=1,4} (|F_c|_i + \Delta)^2$$

$$\Delta = \{[(\Sigma|F_c|)^2 + 4(I_o - \Sigma|F_c|^2)]^{1/2} - \Sigma|F_c|\}/4.$$

The plus sign for the square root was chosen so as not to change the sign of $|F_o|$. The Δ so determined was then assigned each of the four sets of indices and phases to obtain the Fourier map. The largest peaks were around framework atoms in what will be described later as layer No. 9. The map indicated that four O atoms and four Si atoms were misplaced by rotations about certain O–O directions. That the structure of the framework is such as to permit a gross rearrangement of some of the atoms without disrupting the stereochemistry imposed is interesting in its own right and will be discussed later. Repositioning of these atoms and further refinement reduced R to 6·4%. The largest peaks in a difference Fourier map computed at this stage were around Si atoms, suggesting that the electron density around these atoms is somewhat anisotropic. Refinement was terminated at this stage. The final coordinates are listed in Table 1.*

Because of the extraordinarily large number of structural parameters relative to the number of independent intensity data, we feel that further unconstrained least-squares refinement would not have yielded meaningful results. The next logical step, should further refinement of this data be undertaken, would be to allow for anisotropic thermal factors for Si atoms. A still further step might be to separate the O atoms into two populations for thermal refinement: in-layer and between-layer. In monoclinic low tridymite these two groups have significantly different thermal parameters (Baur, 1977).

Discussion of structure

The 320 Si–O distances range from 1·585 to 1·623 Å with an average of 1·606 Å. They are listed in Table 2.

* A list of structure factors has been deposited with the British Library Lending Division as Supplementary Publication No. SUP 33016 (65 pp.). Copies may be obtained through The Executive Secretary, International Union of Crystallography, 13 White Friars, Chester CH1 1NZ, England.

Table 2. Si–O *tetrahedral distances in low tridymite* (Å)

Si atoms are those from Table 1; O atoms are related to those of Table 1 by the symmetry transformations of Table 5. The average Si–O distance is given for each tetrahedron. Estimated standard deviation of an individual distance is approximately 0·005 Å.

ATOM 1	ATOM 2	SYM2	DIS	ATOM 2	SYM2	DIS	AVG
SI(1)1	O(1,2)1	1	1.609	O(1) 1	1	1.614	1.610
	O(1) 2	1	1.612	O(1) 5	1	1.603	
SI(1)2	O(1,2)2	1	1.591	O(1) 3	1	1.606	1.602
	O(1) 4	1	1.616	O(1) 6	1	1.596	
SI(1)3	O(10,1)2	11	1.608	O(1) 5	1	1.614	1.610
	O(1) 7	1	1.603	O(1) 8	1	1.614	
SI(1)4	O(1,2)3	1	1.609	O(1) 8	1	1.616	1.610
	O(1) 9	1	1.609	O(1)11	1	1.606	
SI(1)5	O(10,1)1	9	1.611	O(1) 6	1	1.601	1.609
	O(1) 9	1	1.610	O(1)10	1	1.614	
SI(1)6	O(1,2)4	1	1.607	O(1) 7	2	1.609	1.607
	O(1)10	1	1.616	O(1)12	1	1.597	
SI(1)7	O(10,1)4	11	1.607	O(1) 1	6	1.611	1.609
	O(1) 4	7	1.614	O(1)11	1	1.602	
SI(1)8	O(10,1)3	9	1.604	O(1) 2	6	1.617	1.606
	O(1) 3	6	1.608	O(1)12	1	1.595	
SI(2)1	O(1,2)1	1	1.603	O(2) 1	1	1.606	1.608
	O(2) 2	1	1.609	O(2) 5	1	1.613	
SI(2)2	O(1,2)2	1	1.587	O(2) 3	1	1.616	1.605
	O(2) 4	1	1.607	O(2) 6	1	1.611	
SI(2)3	O(2,3)1	1	1.608	O(2) 5	1	1.605	1.610
	O(2) 7	1	1.607	O(2) 8	1	1.621	
SI(2)4	O(1,2)3	1	1.610	O(2) 8	1	1.613	1.610
	O(2) 9	1	1.603	O(2)11	1	1.612	
SI(2)5	O(2,3)2	1	1.606	O(2) 6	1	1.615	1.609
	O(2) 9	1	1.605	O(2)10	1	1.609	
SI(2)6	O(1,2)4	1	1.608	O(2) 7	2	1.604	1.608
	O(2)10	1	1.621	O(2)12	1	1.601	
SI(2)7	O(2,3)3	1	1.615	O(2) 1	6	1.607	1.611
	O(2) 4	7	1.607	O(2)11	1	1.614	
SI(2)8	O(2,3)4	1	1.607	O(2) 2	6	1.604	1.608
	O(2) 3	6	1.606	O(2)12	1	1.614	
SI(3)1	O(3,4)1	1	1.596	O(3) 1	1	1.609	1.606
	O(3) 2	1	1.611	O(3) 5	1	1.608	
SI(3)2	O(3,4)2	1	1.606	O(3) 3	1	1.605	1.606
	O(3) 4	1	1.609	O(3) 6	1	1.606	
SI(3)3	O(2,3)1	1	1.613	O(3) 5	1	1.609	1.608
	O(3) 7	1	1.603	O(3) 8	1	1.606	
SI(3)4	O(3,4)3	1	1.610	O(3) 8	1	1.606	1.607
	O(3) 9	1	1.609	O(3)11	1	1.601	
SI(3)5	O(2,3)2	1	1.611	O(3) 6	1	1.604	1.608
	O(3) 9	1	1.608	O(3)10	1	1.607	
SI(3)6	O(3,4)4	1	1.615	O(3) 7	2	1.605	1.608
	O(3)10	1	1.604	O(3)12	1	1.607	
SI(3)7	O(2,3)3	1	1.609	O(3) 1	6	1.611	1.607
	O(3) 4	7	1.605	O(3)11	1	1.601	
SI(3)8	O(2,3)4	1	1.602	O(3) 2	6	1.609	1.607
	O(3) 3	6	1.609	O(3)12	1	1.606	
SI(4)1	O(3,4)1	1	1.604	O(4) 1	1	1.601	1.606
	O(4) 2	1	1.607	O(4) 5	1	1.612	
SI(4)2	O(3,4)2	1	1.613	O(4) 3	1	1.608	1.610
	O(4) 4	1	1.609	O(4) 6	1	1.610	
SI(4)3	O(4,5)1	1	1.606	O(4) 5	1	1.608	1.608
	O(4) 7	1	1.616	O(4) 8	1	1.603	
SI(4)4	O(3,4)3	1	1.605	O(4) 8	1	1.609	1.610
	O(4) 9	1	1.618	O(4)11	1	1.607	
SI(4)5	O(4,5)2	1	1.608	O(4) 6	1	1.613	1.610
	O(4) 9	1	1.614	O(4)10	1	1.606	
SI(4)6	O(3,4)4	1	1.608	O(4) 7	2	1.613	1.610
	O(4)10	1	1.612	O(4)12	1	1.607	
SI(4)7	O(4,5)3	1	1.600	O(4) 1	6	1.607	1.606
	O(4) 4	7	1.611	O(4)11	1	1.608	
SI(4)8	O(4,5)4	1	1.591	O(4) 2	6	1.615	1.605
	O(4) 3	6	1.611	O(4)12	1	1.604	
SI(5)1	O(5,6)1	1	1.603	O(5) 1	1	1.613	1.606
	O(5) 2	1	1.611	O(5) 5	1	1.597	
SI(5)2	O(5,6)2	1	1.607	O(5) 3	1	1.607	1.605
	O(5) 4	1	1.611	O(5) 6	1	1.596	
SI(5)3	O(4,5)1	1	1.603	O(5) 5	1	1.603	1.605
	O(5) 7	1	1.613	O(5) 8	1	1.601	
SI(5)4	O(5,6)3	1	1.610	O(5) 8	1	1.606	1.607
	O(5) 9	1	1.610	O(5)11	1	1.601	
SI(5)5	O(4,5)2	1	1.605	O(5) 6	1	1.603	1.605
	O(5) 9	1	1.611	O(5)10	1	1.599	
SI(5)6	O(5,6)4	1	1.609	O(5) 7	2	1.608	1.606
	O(5)10	1	1.604	O(5)12	1	1.604	
SI(5)7	O(4,5)3	1	1.606	O(5) 1	6	1.613	1.606
	O(5) 4	7	1.609	O(5)11	1	1.596	
SI(5)8	O(4,5)4	1	1.594	O(5) 2	6	1.607	1.603
	O(5) 3	6	1.614	O(5)12	1	1.599	

ATOM 1	ATOM 2	SYM2	DIS	ATOM 2	SYM2	DIS	AVG
SI(6)1	O(5,6)1	1	1.606	O(6) 1	1	1.603	1.604
	O(6) 2	1	1.608	O(6) 5	1	1.599	
SI(6)2	O(5,6)2	1	1.607	O(6) 3	1	1.608	1.607
	O(6) 4	1	1.612	O(6) 6	1	1.599	
SI(6)3	O(6,7)1	1	1.589	O(6) 5	1	1.601	1.604
	O(6) 7	1	1.614	O(6) 8	1	1.614	
SI(6)4	O(5,6)3	1	1.610	O(6) 8	1	1.610	1.611
	O(6) 9	1	1.612	O(6)11	1	1.610	
SI(6)5	O(6,7)2	1	1.589	O(6) 6	1	1.601	1.605
	O(6) 9	1	1.621	O(6)10	1	1.607	
SI(6)6	O(5,6)4	1	1.609	O(6) 7	2	1.609	1.608
	O(6)10	1	1.612	O(6)12	1	1.604	
SI(6)7	O(6,7)3	1	1.612	O(6) 1	6	1.598	1.608
	O(6) 4	7	1.610	O(6)11	1	1.611	
SI(6)8	O(6,7)4	1	1.611	O(6) 2	6	1.607	1.607
	O(6) 3	6	1.602	O(6)12	1	1.609	
SI(7)1	O(7,8)1	1	1.600	O(7) 1	1	1.603	1.606
	O(7) 2	1	1.611	O(7) 5	1	1.612	
SI(7)2	O(7,8)2	1	1.609	O(7) 3	1	1.608	1.610
	O(7) 4	1	1.614	O(7) 6	1	1.608	
SI(7)3	O(6,7)1	1	1.599	O(7) 5	1	1.605	1.604
	O(7) 7	1	1.612	O(7) 8	1	1.602	
SI(7)4	O(7,8)3	1	1.606	O(7) 8	1	1.604	1.607
	O(7) 9	1	1.616	O(7)11	1	1.604	
SI(7)5	O(6,7)2	1	1.595	O(7) 6	1	1.618	1.605
	O(7) 9	1	1.607	O(7)10	1	1.600	
SI(7)6	O(7,8)4	1	1.604	O(7) 7	2	1.611	1.608
	O(7)10	1	1.601	O(7)12	1	1.614	
SI(7)7	O(6,7)3	1	1.604	O(7) 1	6	1.605	1.607
	O(7) 4	7	1.609	O(7)11	1	1.610	
SI(7)8	O(6,7)4	1	1.603	O(7) 2	6	1.615	1.609
	O(7) 3	6	1.610	O(7)12	1	1.609	
SI(8)1	O(7,8)1	1	1.600	O(8) 1	1	1.606	1.606
	O(8) 2	1	1.610	O(8) 5	1	1.611	
SI(8)2	O(7,8)2	1	1.608	O(8) 3	1	1.604	1.607
	O(8) 4	1	1.611	O(8) 6	1	1.605	
SI(8)3	O(8,9)1	1	1.614	O(8) 5	1	1.614	1.611
	O(8) 7	1	1.608	O(8) 8	1	1.606	
SI(8)4	O(7,8)3	1	1.611	O(8) 8	1	1.613	1.608
	O(8) 9	1	1.605	O(8)11	1	1.604	
SI(8)5	O(8,9)2	1	1.617	O(8) 6	1	1.605	1.608
	O(8) 9	1	1.608	O(8)10	1	1.604	
SI(8)6	O(7,8)4	1	1.611	O(8) 7	2	1.610	1.607
	O(8)10	1	1.605	O(8)12	1	1.600	
SI(8)7	O(8,9)3	1	1.602	O(8) 1	6	1.611	1.607
	O(8) 4	7	1.605	O(8)11	1	1.610	
SI(8)8	O(8,9)4	1	1.590	O(8) 2	6	1.605	1.605
	O(8) 3	6	1.614	O(8)12	1	1.609	
SI(9)1	O(10,9)1	1	1.599	O(9) 1	1	1.607	1.607
	O(9) 2	1	1.609	O(9) 5	1	1.612	
SI(9)2	O(10,9)2	1	1.595	O(9) 3	1	1.623	1.607
	O(9) 4	1	1.610	O(9) 6	1	1.601	
SI(9)3	O(8,9)1	1	1.605	O(9) 5	1	1.603	1.607
	O(9) 7	1	1.602	O(9) 8	1	1.620	
SI(9)4	O(10,9)3	1	1.591	O(9) 8	1	1.605	1.603
	O(9) 9	1	1.598	O(9)11	1	1.620	
SI(9)5	O(8,9)2	1	1.608	O(9) 6	1	1.617	1.607
	O(9) 9	1	1.595	O(9)10	1	1.609	
SI(9)6	O(10,9)4	1	1.606	O(9) 7	2	1.602	1.607
	O(9)10	1	1.619	O(9)12	1	1.602	
SI(9)7	O(8,9)3	1	1.607	O(9) 1	6	1.619	1.609
	O(9) 4	7	1.608	O(9)11	1	1.602	
SI(9)8	O(8,9)4	1	1.596	O(9) 2	6	1.605	1.606
	O(9) 3	6	1.610	O(9)12	1	1.614	
SI(10)1	O(10,9)1	1	1.611	O(10) 1	1	1.603	1.605
	O(10) 2	1	1.605	O(10) 5	1	1.601	
SI(10)2	O(10,9)2	1	1.604	O(10) 3	1	1.602	1.604
	O(10) 4	1	1.602	O(10) 6	1	1.607	
SI(10)3	O(10,1)1	1	1.606	O(10) 5	1	1.609	1.608
	O(10) 7	1	1.613	O(10) 8	1	1.605	
SI(10)4	O(10,9)3	1	1.585	O(10) 8	1	1.615	1.603
	O(10) 9	1	1.608	O(10)11	1	1.606	
SI(10)5	O(10,1)2	1	1.609	O(10) 6	1	1.606	1.609
	O(10) 9	1	1.612	O(10)10	1	1.609	
SI(10)6	O(10,9)4	1	1.598	O(10) 7	2	1.603	1.606
	O(10)10	1	1.617	O(10)12	1	1.607	
SI(10)7	O(10,1)3	1	1.611	O(10) 1	6	1.604	1.603
	O(10) 4	7	1.601	O(10)11	1	1.598	
SI(10)8	O(10,1)4	1	1.610	O(10) 2	6	1.600	1.606
	O(10) 3	6	1.613	O(10)12	1	1.601	

The average Si–O values for each of the 80 tetrahedra range from 1·602 to 1·611 Å. The O–O distances and O–Si–O angles of the tetrahedra are given in Table 3; the 480 O–O distances range from 2·57 to 2·69 Å with an average value of 2·63 Å. The accuracy of the atomic coordinates was not estimated from the solution to the normal equations, since the inverse-matrix elements were not calculated by the version of the CG procedure then being used. The pseudosymmetry present, but not imposed on the structure by the space group or the distance restraints, suggests, along with the low R value and good stereochemistry, that the standard deviations in atomic positions are ~0·02 Å. Taking into account the distance constraints applied and the expected and

Table 3. O—O *distances* (Å) *and* O—Si—O *angles* (°) *within tetrahedra in low tridymite*

Conventions are as in Table 2. Estimated standard deviation of an individual distance is approximately 0·02 Å.

ATOM 1	ATOM 2	SYM2	ATOM 3	SYM3	DIS	ANG	AVG
SI(1)1	O(1,2)1	1	O(1) 1	1	2.614	108.4	2.628
	O(1,2)1	1	O(1) 2	1	2.622	109.0	
	O(1,2)1	1	O(1) 5	1	2.614	109.0	
	O(1) 1	1	O(1) 2	1	2.617	108.5	
	O(1) 1	1	O(1) 5	1	2.657	111.3	
	O(1) 2	1	O(1) 5	1	2.644	110.6	
SI(1)2	O(1,2)2	1	O(1) 3	1	2.626	110.4	2.616
	O(1,2)2	1	O(1) 4	1	2.585	107.5	
	O(1,2)2	1	O(1) 6	1	2.595	109.0	
	O(1) 3	1	O(1) 4	1	2.610	108.2	
	O(1) 3	1	O(1) 6	1	2.661	112.4	
	O(1) 4	1	O(1) 6	1	2.619	109.3	
SI(1)3	O(10,1)2	11	O(1) 5	1	2.627	109.2	2.628
	O(10,1)2	11	O(1) 7	1	2.644	110.9	
	O(10,1)2	11	O(1) 8	1	2.613	108.4	
	O(1) 5	1	O(1) 7	1	2.622	109.2	
	O(1) 5	1	O(1) 8	1	2.582	106.2	
	O(1) 7	1	O(1) 8	1	2.679	112.8	
SI(1)4	O(1,2)3	1	O(1) 8	1	2.613	108.2	2.629
	O(1,2)3	1	O(1) 9	1	2.654	111.1	
	O(1,2)3	1	O(1)11	1	2.632	109.9	
	O(1) 8	1	O(1) 9	1	2.654	110.8	
	O(1) 8	1	O(1)11	1	2.606	108.0	
	O(1) 9	1	O(1)11	1	2.614	108.8	
SI(1)5	O(10,1)1	9	O(1) 6	1	2.625	109.7	2.627
	O(10,1)1	9	O(1) 9	1	2.644	110.3	
	O(10,1)1	9	O(1)10	1	2.616	108.4	
	O(1) 6	1	O(1) 9	1	2.624	109.6	
	O(1) 6	1	O(1)10	1	2.586	107.1	
	O(1) 9	1	O(1)10	1	2.668	111.7	
SI(1)6	O(1,2)4	1	O(1) 7	2	2.624	109.4	2.624
	O(1,2)4	1	O(1)10	1	2.611	108.3	
	O(1,2)4	1	O(1)12	1	2.653	111.8	
	O(1) 7	2	O(1)10	1	2.652	110.7	
	O(1) 7	2	O(1)12	1	2.605	108.7	
	O(1)10	1	O(1)12	1	2.599	108.0	
SI(1)7	O(10,1)4	11	O(1) 1	6	2.629	109.6	2.627
	O(10,1)4	11	O(1) 4	7	2.625	109.2	
	O(10,1)4	11	O(1)11	1	2.617	109.3	
	O(1) 1	6	O(1) 4	7	2.609	108.0	
	O(1) 1	6	O(1)11	1	2.618	109.2	
	O(1) 4	7	O(1)11	1	2.661	111.7	
SI(1)8	O(10,1)3	9	O(1) 2	6	2.638	110.0	2.622
	O(10,1)3	9	O(1) 3	6	2.630	110.0	
	O(10,1)3	9	O(1)12	1	2.596	108.5	
	O(1) 2	6	O(1) 3	6	2.620	108.7	
	O(1) 2	6	O(1)12	1	2.644	110.8	
	O(1) 3	6	O(1)12	1	2.606	108.9	
SI(2)1	O(1,2)1	1	O(2) 1	1	2.643	110.9	2.625
	O(1,2)1	1	O(2) 2	1	2.641	110.7	
	O(1,2)1	1	O(2) 5	1	2.645	110.6	
	O(2) 1	1	O(2) 2	1	2.615	108.9	
	O(2) 1	1	O(2) 5	1	2.600	107.7	
	O(2) 2	1	O(2) 5	1	2.607	108.0	
SI(2)2	O(1,2)2	1	O(2) 3	1	2.587	107.7	2.621
	O(1,2)2	1	O(2) 4	1	2.620	110.2	
	O(1,2)2	1	O(2) 6	1	2.647	111.7	
	O(2) 3	1	O(2) 4	1	2.639	109.9	
	O(2) 3	1	O(2) 6	1	2.601	107.5	
	O(2) 4	1	O(2) 6	1	2.632	109.8	
SI(2)3	O(2,3)1	1	O(2) 5	1	2.670	112.4	2.629
	O(2,3)1	1	O(2) 7	1	2.621	109.2	
	O(2,3)1	1	O(2) 8	1	2.623	108.7	
	O(2) 5	1	O(2) 7	1	2.647	111.0	
	O(2) 5	1	O(2) 8	1	2.603	107.6	
	O(2) 7	1	O(2) 8	1	2.609	107.8	
SI(2)4	O(1,2)3	1	O(2) 8	1	2.630	109.4	2.628
	O(1,2)3	1	O(2) 9	1	2.590	107.5	
	O(1,2)3	1	O(2)11	1	2.637	109.8	
	O(2) 8	1	O(2) 9	1	2.661	111.7	
	O(2) 8	1	O(2)11	1	2.617	108.5	
	O(2) 9	1	O(2)11	1	2.633	110.0	
SI(2)5	O(2,3)2	1	O(2) 6	1	2.628	109.3	2.627
	O(2,3)2	1	O(2) 9	1	2.613	109.0	
	O(2,3)2	1	O(2)10	1	2.662	111.8	
	O(2) 6	1	O(2) 9	1	2.622	109.0	
	O(2) 6	1	O(2)10	1	2.603	107.7	
	O(2) 9	1	O(2)10	1	2.632	110.0	

ATOM 1	ATOM 2	SYM2	ATOM 3	SYM3	DIS	ANG	AVG
SI(2)6	O(1,2)4	1	O(2) 7	2	2.620	109.4	2.625
	O(1,2)4	1	O(2)10	1	2.624	108.7	
	O(1,2)4	1	O(2)12	1	2.625	109.8	
	O(2) 7	2	O(2)10	1	2.592	107.0	
	O(2) 7	2	O(2)12	1	2.688	114.1	
	O(2)10	1	O(2)12	1	2.602	107.8	
SI(2)7	O(2,3)3	1	O(2) 1	6	2.633	109.6	2.630
	O(2,3)3	1	O(2) 4	7	2.624	109.1	
	O(2,3)3	1	O(2)11	1	2.629	109.0	
	O(2) 1	6	O(2) 4	7	2.607	108.4	
	O(2) 1	6	O(2)11	1	2.616	108.6	
	O(2) 4	7	O(2)11	1	2.673	112.2	
SI(2)8	O(2,3)4	1	O(2) 2	6	2.633	110.2	2.625
	O(2,3)4	1	O(2) 3	6	2.628	109.8	
	O(2,3)4	1	O(2)12	1	2.604	107.9	
	O(2) 2	6	O(2) 3	6	2.660	112.0	
	O(2) 2	6	O(2)12	1	2.603	108.0	
	O(2) 3	6	O(2)12	1	2.621	109.0	
SI(3)1	O(3,4)1	1	O(3) 1	1	2.659	112.2	2.622
	O(3,4)1	1	O(3) 2	1	2.614	109.3	
	O(3,4)1	1	O(3) 5	1	2.597	108.3	
	O(3) 1	1	O(3) 2	1	2.598	107.6	
	O(3) 1	1	O(3) 5	1	2.644	110.6	
	O(3) 2	1	O(3) 5	1	2.618	108.9	
SI(3)2	O(3,4)2	1	O(3) 3	1	2.651	111.4	2.622
	O(3,4)2	1	O(3) 4	1	2.617	109.0	
	O(3,4)2	1	O(3) 6	1	2.605	108.5	
	O(3) 3	1	O(3) 4	1	2.614	108.9	
	O(3) 3	1	O(3) 6	1	2.652	111.4	
	O(3) 4	1	O(3) 6	1	2.594	107.6	
SI(3)3	O(2,3)1	1	O(3) 5	1	2.615	108.5	2.625
	O(2,3)1	1	O(3) 7	1	2.625	109.4	
	O(2,3)1	1	O(3) 8	1	2.596	107.5	
	O(3) 5	1	O(3) 7	1	2.637	110.3	
	O(3) 5	1	O(3) 8	1	2.640	110.4	
	O(3) 7	1	O(3) 8	1	2.639	110.7	
SI(3)4	O(3,4)3	1	O(3) 8	1	2.625	109.4	2.624
	O(3,4)3	1	O(3) 9	1	2.620	108.9	
	O(3,4)3	1	O(3)11	1	2.616	109.1	
	O(3) 8	1	O(3) 9	1	2.611	108.6	
	O(3) 8	1	O(3)11	1	2.635	110.5	
	O(3) 9	1	O(3)11	1	2.634	110.3	
SI(3)5	O(2,3)2	1	O(3) 6	1	2.623	109.3	2.625
	O(2,3)2	1	O(3) 9	1	2.628	109.4	
	O(2,3)2	1	O(3)10	1	2.587	107.0	
	O(3) 6	1	O(3) 9	1	2.627	109.7	
	O(3) 6	1	O(3)10	1	2.647	111.1	
	O(3) 9	1	O(3)10	1	2.638	110.3	
SI(3)6	O(3,4)4	1	O(3) 7	2	2.591	107.2	2.625
	O(3,4)4	1	O(3)10	1	2.627	109.4	
	O(3,4)4	1	O(3)12	1	2.617	108.0	
	O(3) 7	2	O(3)10	1	2.638	110.6	
	O(3) 7	2	O(3)12	1	2.636	110.3	
	O(3)10	1	O(3)12	1	2.641	110.7	
SI(3)7	O(2,3)3	1	O(3) 1	6	2.637	110.0	2.623
	O(2,3)3	1	O(3) 4	7	2.651	111.1	
	O(2,3)3	1	O(3)11	1	2.617	109.2	
	O(3) 1	6	O(3) 4	7	2.610	108.5	
	O(3) 1	6	O(3)11	1	2.577	106.7	
	O(3) 4	7	O(3)11	1	2.646	111.2	
SI(3)8	O(2,3)4	1	O(3) 2	6	2.643	110.8	2.623
	O(2,3)4	1	O(3) 3	6	2.609	108.6	
	O(2,3)4	1	O(3)12	1	2.615	109.2	
	O(3) 2	6	O(3) 3	6	2.619	109.0	
	O(3) 2	6	O(3)12	1	2.655	111.4	
	O(3) 3	6	O(3)12	1	2.599	107.8	
SI(4)1	O(3,4)1	1	O(4) 1	1	2.609	109.0	2.622
	O(3,4)1	1	O(4) 2	1	2.617	109.2	
	O(3,4)1	1	O(4) 5	1	2.599	107.8	
	O(4) 1	1	O(4) 2	1	2.665	112.4	
	O(4) 1	1	O(4) 5	1	2.622	109.4	
	O(4) 2	1	O(4) 5	1	2.621	109.0	
SI(4)2	O(3,4)2	1	O(4) 3	1	2.605	108.0	2.629
	O(3,4)2	1	O(4) 4	1	2.636	109.7	
	O(3,4)2	1	O(4) 6	1	2.617	108.6	
	O(4) 3	1	O(4) 4	1	2.616	108.8	
	O(4) 3	1	O(4) 6	1	2.681	112.8	
	O(4) 4	1	O(4) 6	1	2.620	108.9	

experimental distributions of interatomic distances, we estimate that the standard deviations for individual distances are as follows: Si—O 0·005; O—O 0·02; Si—Si 0·03 Å. The isotropic B for the Si atoms refined to a value of 0·61 Å^2. The refined values for the axes describing the anisotropic ellipsoid of the O atoms are 0·60 Å^2 for the axis parallel to the line connecting the bridged Si atoms, 2·20 Å^2 for the axis perpendicular to the Si—O—Si plane, and 1·65 Å^2 for the third axis. The Si—Si distances and Si—O—Si angles are given in Table 4, with the symmetry transformations used to generate Tables 2–4 given in Table 5.

The structure will be discussed in terms of layers of tetrahedra parallel to (001). Since the structure is a framework, such a description, of course, is somewhat arbitrary. There are, however, several reasons for

Table 3 (*cont.*)

ATOM 1	ATOM 2	SYM2	ATOM 3	SYM3	DIS	ANG	AVG
SI(4)3	O(4,5)1	1	O(4) 5	1	2.602	108.1	2.625
	O(4,5)1	1	O(4) 7	1	2.629	109.4	
	O(4,5)1	1	O(4) 8	1	2.612	109.0	
	O(4) 5	1	O(4) 7	1	2.595	107.2	
	O(4) 5	1	O(4) 8	1	2.693	114.0	
	O(4) 7	1	O(4) 8	1	2.621	109.0	
SI(4)4	O(3,4)3	1	O(4) 8	1	2.617	109.0	2.628
	O(3,4)3	1	O(4) 9	1	2.619	108.7	
	O(3,4)3	1	O(4)11	1	2.666	112.2	
	O(4) 8	1	O(4) 9	1	2.633	109.4	
	O(4) 8	1	O(4)11	1	2.631	109.8	
	O(4) 9	1	O(4)11	1	2.603	107.7	
SI(4)5	O(4,5)2	1	O(4) 6	1	2.620	108.8	2.630
	O(4,5)2	1	O(4) 9	1	2.612	108.3	
	O(4,5)2	1	O(4)10	1	2.614	108.8	
	O(4) 6	1	O(4) 9	1	2.616	108.3	
	O(4) 6	1	O(4)10	1	2.644	110.5	
	O(4) 9	1	O(4)10	1	2.672	112.1	
SI(4)6	O(3,4)4	1	O(4) 7	2	2.668	111.9	2.629
	O(3,4)4	1	O(4)10	1	2.601	107.7	
	O(3,4)4	1	O(4)12	1	2.643	110.6	
	O(4) 7	2	O(4)10	1	2.630	109.3	
	O(4) 7	2	O(4)12	1	2.604	108.0	
	O(4)10	1	O(4)12	1	2.627	109.4	
SI(4)7	O(4,5)3	1	O(4) 1	6	2.618	109.5	2.623
	O(4,5)3	1	O(4) 4	7	2.647	111.1	
	O(4,5)3	1	O(4)11	1	2.645	111.1	
	O(4) 1	6	O(4) 4	7	2.607	108.2	
	O(4) 1	6	O(4)11	1	2.608	108.5	
	O(4) 4	7	O(4)11	1	2.612	108.4	
SI(4)8	O(4,5)4	1	O(4) 2	6	2.588	107.7	2.621
	O(4,5)4	1	O(4) 3	6	2.584	107.6	
	O(4,5)4	1	O(4)12	1	2.660	112.7	
	O(4) 2	6	O(4) 3	6	2.645	110.1	
	O(4) 2	6	O(4)12	1	2.606	108.1	
	O(4) 3	6	O(4)12	1	2.643	110.6	
SI(5)1	O(5,6)1	1	O(5) 1	1	2.641	110.4	2.622
	O(5,6)1	1	O(5) 2	1	2.590	107.4	
	O(5,6)1	1	O(5) 5	1	2.621	110.0	
	O(5) 1	1	O(5) 2	1	2.606	107.9	
	O(5) 1	1	O(5) 5	1	2.667	112.4	
	O(5) 2	1	O(5) 5	1	2.606	108.7	
SI(5)2	O(5,6)2	1	O(5) 3	1	2.622	109.3	2.621
	O(5,6)2	1	O(5) 4	1	2.598	107.6	
	O(5,6)2	1	O(5) 6	1	2.610	109.2	
	O(5) 3	1	O(5) 4	1	2.607	108.2	
	O(5) 3	1	O(5) 6	1	2.670	112.9	
	O(5) 4	1	O(5) 6	1	2.619	109.5	
SI(5)3	O(4,5)1	1	O(5) 5	1	2.634	110.5	2.620
	O(4,5)1	1	O(5) 7	1	2.620	109.1	
	O(4,5)1	1	O(5) 8	1	2.644	111.2	
	O(5) 5	1	O(5) 7	1	2.582	106.8	
	O(5) 5	1	O(5) 8	1	2.624	110.0	
	O(5) 7	1	O(5) 8	1	2.619	109.2	
SI(5)4	O(5,6)3	1	O(5) 8	1	2.623	109.3	2.624
	O(5,6)3	1	O(5) 9	1	2.613	108.5	
	O(5,6)3	1	O(5)11	1	2.652	111.4	
	O(5) 8	1	O(5) 9	1	2.631	109.8	
	O(5) 8	1	O(5)11	1	2.588	107.6	
	O(5) 9	1	O(5)11	1	2.635	110.3	
SI(5)5	O(4,5)2	1	O(5) 6	1	2.634	110.4	2.620
	O(4,5)2	1	O(5) 9	1	2.628	109.6	
	O(4,5)2	1	O(5)10	1	2.642	111.1	
	O(5) 6	1	O(5) 9	1	2.583	107.0	
	O(5) 6	1	O(5)10	1	2.626	110.2	
	O(5) 9	1	O(5)10	1	2.607	108.6	
SI(5)6	O(5,6)4	1	O(5) 7	2	2.620	109.1	2.623
	O(5,6)4	1	O(5)10	1	2.636	110.3	
	O(5,6)4	1	O(5)12	1	2.633	110.1	
	O(5) 7	2	O(5)10	1	2.648	111.0	
	O(5) 7	2	O(5)12	1	2.626	109.7	
	O(5)10	1	O(5)12	1	2.575	106.7	
SI(5)7	O(4,5)3	1	O(5) 1	6	2.606	108.1	2.622
	O(4,5)3	1	O(5) 4	7	2.614	108.9	
	O(4,5)3	1	O(5)11	1	2.610	109.2	
	O(5) 1	6	O(5) 4	7	2.606	108.0	
	O(5) 1	6	O(5)11	1	2.619	109.4	
	O(5) 4	7	O(5)11	1	2.676	113.2	

ATOM 1	ATOM 2	SYM2	ATOM 3	SYM3	DIS	ANG	AVG
SI(5)8	O(4,5)4	1	O(5) 2	6	2.628	110.4	2.617
	O(4,5)4	1	O(5) 3	6	2.559	105.8	
	O(4,5)4	1	O(5)12	1	2.592	108.6	
	O(5) 2	6	O(5) 3	6	2.622	109.0	
	O(5) 2	6	O(5)12	1	2.677	113.3	
	O(5) 3	6	O(5)12	1	2.624	109.6	
SI(6)1	O(5,6)1	1	O(6) 1	1	2.579	107.0	2.619
	O(5,6)1	1	O(6) 2	1	2.627	109.7	
	O(5,6)1	1	O(6) 5	1	2.610	109.1	
	O(6) 1	1	O(6) 2	1	2.635	110.3	
	O(6) 1	1	O(6) 5	1	2.628	110.3	
	O(6) 2	1	O(6) 5	1	2.635	110.5	
SI(6)2	O(5,6)2	1	O(6) 3	1	2.604	108.2	2.623
	O(5,6)2	1	O(6) 4	1	2.604	108.0	
	O(5,6)2	1	O(6) 6	1	2.625	109.9	
	O(6) 3	1	O(6) 4	1	2.640	110.1	
	O(6) 3	1	O(6) 6	1	2.632	110.3	
	O(6) 4	1	O(6) 6	1	2.635	110.3	
SI(6)3	O(6,7)1	1	O(6) 5	1	2.643	111.9	2.619
	O(6,7)1	1	O(6) 7	1	2.605	108.8	
	O(6,7)1	1	O(6) 8	1	2.649	111.5	
	O(6) 5	1	O(6) 7	1	2.596	107.7	
	O(6) 5	1	O(6) 8	1	2.610	108.5	
	O(6) 7	1	O(6) 8	1	2.615	108.2	
SI(6)4	O(5,6)3	1	O(6) 8	1	2.621	109.0	2.630
	O(5,6)3	1	O(6) 9	1	2.654	110.9	
	O(5,6)3	1	O(6)11	1	2.623	109.1	
	O(6) 8	1	O(6) 9	1	2.609	108.1	
	O(6) 8	1	O(6)11	1	2.635	109.8	
	O(6) 9	1	O(6)11	1	2.639	110.0	
SI(6)5	O(6,7)2	1	O(6) 6	1	2.648	112.2	2.619
	O(6,7)2	1	O(6) 9	1	2.587	107.4	
	O(6,7)2	1	O(6)10	1	2.655	112.3	
	O(6) 6	1	O(6) 9	1	2.590	107.0	
	O(6) 6	1	O(6)10	1	2.632	110.3	
	O(6) 9	1	O(6)10	1	2.602	107.4	
SI(6)6	O(5,6)4	1	O(6) 7	2	2.663	111.7	2.626
	O(5,6)4	1	O(6)10	1	2.602	107.8	
	O(5,6)4	1	O(6)12	1	2.627	109.7	
	O(6) 7	2	O(6)10	1	2.615	108.6	
	O(6) 7	2	O(6)12	1	2.643	110.7	
	O(6)10	1	O(6)12	1	2.607	108.3	
SI(6)7	O(6,7)3	1	O(6) 1	6	2.621	109.5	2.625
	O(6,7)3	1	O(6) 4	7	2.621	108.9	
	O(6,7)3	1	O(6)11	1	2.627	109.2	
	O(6) 1	6	O(6) 4	7	2.643	111.0	
	O(6) 1	6	O(6)11	1	2.625	109.8	
	O(6) 4	7	O(6)11	1	2.616	108.6	
SI(6)8	O(6,7)4	1	O(6) 2	6	2.624	109.2	2.624
	O(6,7)4	1	O(6) 3	6	2.621	109.3	
	O(6,7)4	1	O(6)12	1	2.596	107.4	
	O(6) 2	6	O(6) 3	6	2.656	111.8	
	O(6) 2	6	O(6)12	1	2.622	109.3	
	O(6) 3	6	O(6)12	1	2.626	109.7	
SI(7)1	O(7,8)1	1	O(7) 1	1	2.613	109.4	2.622
	O(7,8)1	1	O(7) 2	1	2.635	110.3	
	O(7,8)1	1	O(7) 5	1	2.596	107.9	
	O(7) 1	1	O(7) 2	1	2.672	112.5	
	O(7) 1	1	O(7) 5	1	2.608	108.4	
	O(7) 2	1	O(7) 5	1	2.610	108.2	
SI(7)2	O(7,8)2	1	O(7) 3	1	2.600	107.9	2.628
	O(7,8)2	1	O(7) 4	1	2.652	110.7	
	O(7,8)2	1	O(7) 6	1	2.629	109.6	
	O(7) 3	1	O(7) 4	1	2.610	108.2	
	O(7) 3	1	O(7) 6	1	2.662	111.8	
	O(7) 4	1	O(7) 6	1	2.617	108.6	
SI(7)3	O(6,7)1	1	O(7) 5	1	2.604	108.7	2.620
	O(6,7)1	1	O(7) 7	1	2.629	109.9	
	O(6,7)1	1	O(7) 8	1	2.601	108.7	
	O(7) 5	1	O(7) 7	1	2.587	107.1	
	O(7) 5	1	O(7) 8	1	2.680	113.4	
	O(7) 7	1	O(7) 8	1	2.617	109.0	
SI(7)4	O(7,8)3	1	O(7) 8	1	2.606	108.6	2.624
	O(7,8)3	1	O(7) 9	1	2.607	108.0	
	O(7,8)3	1	O(7)11	1	2.672	112.7	
	O(7) 8	1	O(7) 9	1	2.614	108.6	
	O(7) 8	1	O(7)11	1	2.651	111.5	
	O(7) 9	1	O(7)11	1	2.595	107.4	

choosing this description. The most important among these are (1) the internal symmetry of the layers and how this symmetry is related to possible ambiguities in the structure, (2) the layer-like morphology and cleavage and (3) streaking parallel to **c*** perhaps related to layer-stacking faults. The ten layers in the asymmetric unit are illustrated in Fig. 1.

To an average accuracy of about 0·1 Å, the structure may be thought of as composed of four different types of layers in the sequence illustrated in Fig. 2. Approximate transformations relating the layers are listed in Table 6.

It may be noted that the projections of the basal (in-layer as opposed to those shared by adjacent layers) O atoms on the *xy* plane are nearly identical for all layers. In order to bring the projections of what will be described as the *B* layers into near-coincidence with the others, it is necessary to rotate about **c** by 60° in addition to the necessary reflections and translations concerning *x* and *y*.

A most remarkable pseudosymmetry possessed by the *A*, *C* and *D*-type layers is their near-periodicity of *a*/2, (*b*/2) (Table 6). As a result, the 32 Si atoms and the 48 in-layer O atoms of the *B*-type layers are the

Table 3 (*cont.*)

ATOM 1	ATOM 2	SYM2	ATOM 3	SYM3	DIS	ANG	AVG
SI(7)5	O(6,7)2	1	O(7) 6	1	2.620	109.3	2.621
	O(6,7)2	1	O(7) 9	1	2.626	110.2	
	O(6,7)2	1	O(7)10	1	2.587	108.1	
	O(7) 6	1	O(7) 9	1	2.588	106.7	
	O(7) 6	1	O(7)10	1	2.625	109.3	
	O(7) 9	1	O(7)10	1	2.678	113.2	
SI(7)6	O(7,8)4	1	O(7) 7	2	2.673	112.5	2.625
	O(7,8)4	1	O(7)10	1	2.606	108.8	
	O(7,8)4	1	O(7)12	1	2.628	109.5	
	O(7) 7	2	O(7)10	1	2.616	109.1	
	O(7) 7	2	O(7)12	1	2.595	107.1	
	O(7)10	1	O(7)12	1	2.629	109.8	
SI(7)7	O(6,7)3	1	O(7) 1	6	2.633	110.2	2.624
	O(6,7)3	1	O(7) 4	7	2.661	111.8	
	O(6,7)3	1	O(7)11	1	2.614	108.8	
	O(7) 1	6	O(7) 4	7	2.628	109.7	
	O(7) 1	6	O(7)11	1	2.601	108.0	
	O(7) 4	7	O(7)11	1	2.605	108.1	
SI(7)8	O(6,7)4	1	O(7) 2	6	2.626	109.4	2.628
	O(6,7)4	1	O(7) 3	6	2.620	109.2	
	O(6,7)4	1	O(7)12	1	2.665	112.1	
	O(7) 2	6	O(7) 3	6	2.615	108.3	
	O(7) 2	6	O(7)12	1	2.602	107.7	
	O(7) 3	6	O(7)12	1	2.638	110.1	
SI(8)1	O(7,8)1	1	O(8) 1	1	2.662	112.3	2.623
	O(7,8)1	1	O(8) 2	1	2.589	107.6	
	O(7,8)1	1	O(8) 5	1	2.594	107.8	
	O(8) 1	1	O(8) 2	1	2.604	108.2	
	O(8) 1	1	O(8) 5	1	2.651	111.1	
	O(8) 2	1	O(8) 5	1	2.636	109.9	
SI(8)2	O(7,8)2	1	O(8) 3	1	2.656	111.6	2.624
	O(7,8)2	1	O(8) 4	1	2.606	108.1	
	O(7,8)2	1	O(8) 6	1	2.636	110.2	
	O(8) 3	1	O(8) 4	1	2.607	108.4	
	O(8) 3	1	O(8) 6	1	2.636	110.4	
	O(8) 4	1	O(8) 6	1	2.602	108.0	
SI(8)3	O(8,9)1	1	O(8) 5	1	2.599	107.3	2.629
	O(8,9)1	1	O(8) 7	1	2.612	108.4	
	O(8,9)1	1	O(8) 8	1	2.623	109.1	
	O(8) 5	1	O(8) 7	1	2.637	109.9	
	O(8) 5	1	O(8) 8	1	2.648	110.7	
	O(8) 7	1	O(8) 8	1	2.657	111.5	
SI(8)4	O(7,8)3	1	O(8) 8	1	2.604	107.7	2.625
	O(7,8)3	1	O(8) 9	1	2.609	108.5	
	O(7,8)3	1	O(8)11	1	2.605	108.2	
	O(8) 8	1	O(8) 9	1	2.628	109.6	
	O(8) 8	1	O(8)11	1	2.642	110.4	
	O(8) 9	1	O(8)11	1	2.666	112.4	
SI(8)5	O(8,9)2	1	O(8) 6	1	2.612	108.4	2.626
	O(8,9)2	1	O(8) 9	1	2.642	110.0	
	O(8,9)2	1	O(8)10	1	2.603	107.8	
	O(8) 6	1	O(8) 9	1	2.623	109.4	
	O(8) 6	1	O(8)10	1	2.653	111.6	
	O(8) 9	1	O(8)10	1	2.626	109.6	
SI(8)6	O(7,8)4	1	O(8) 7	2	2.579	106.4	2.623
	O(7,8)4	1	O(8)10	1	2.616	108.8	
	O(7,8)4	1	O(8)12	1	2.623	109.6	
	O(8) 7	2	O(8)10	1	2.629	109.7	
	O(8) 7	2	O(8)12	1	2.663	112.2	
	O(8)10	1	O(8)12	1	2.628	110.1	
SI(8)7	O(8,9)3	1	O(8) 1	6	2.633	110.1	2.624
	O(8,9)3	1	O(8) 4	7	2.669	112.7	
	O(8,9)3	1	O(8)11	1	2.604	108.3	
	O(8) 1	6	O(8) 4	7	2.599	107.8	
	O(8) 1	6	O(8)11	1	2.608	108.2	
	O(8) 4	7	O(8)11	1	2.630	109.8	
SI(8)8	O(8,9)4	1	O(8) 2	6	2.670	113.4	2.619
	O(8,9)4	1	O(8) 3	6	2.606	108.8	
	O(8,9)4	1	O(8)12	1	2.615	109.6	
	O(8) 2	6	O(8) 3	6	2.607	108.2	
	O(8) 2	6	O(8)12	1	2.633	110.0	
	O(8) 3	6	O(8)12	1	2.584	106.6	
SI(9)1	O(10,9)1	1	O(9) 1	1	2.674	113.0	2.623
	O(10,9)1	1	O(9) 2	1	2.613	109.1	
	O(10,9)1	1	O(9) 5	1	2.620	109.3	
	O(9) 1	1	O(9) 2	1	2.628	109.6	
	O(9) 1	1	O(9) 5	1	2.617	108.8	
	O(9) 2	1	O(9) 5	1	2.587	106.9	
SI(9)2	O(10,9)2	1	O(9) 3	1	2.571	106.1	2.622
	O(10,9)2	1	O(9) 4	1	2.606	108.8	
	O(10,9)2	1	O(9) 6	1	2.682	114.1	
	O(9) 3	1	O(9) 4	1	2.596	106.8	
	O(9) 3	1	O(9) 6	1	2.602	107.6	
	O(9) 4	1	O(9) 6	1	2.677	112.9	

ATOM 1	ATOM 2	SYM2	ATOM 3	SYM3	DIS	ANG	AVG
SI(9)3	O(8,9)1	1	O(9) 5	1	2.665	112.4	2.624
	O(8,9)1	1	O(9) 7	1	2.629	110.1	
	O(8,9)1	1	O(9) 8	1	2.605	107.8	
	O(9) 5	1	O(9) 7	1	2.650	111.6	
	O(9) 5	1	O(9) 8	1	2.593	107.2	
	O(9) 7	1	O(9) 8	1	2.600	107.6	
SI(9)4	O(10,9)3	1	O(9) 8	1	2.661	112.7	2.616
	O(10,9)3	1	O(9) 9	1	2.575	107.7	
	O(10,9)3	1	O(9)11	1	2.568	106.2	
	O(9) 8	1	O(9) 9	1	2.690	114.3	
	O(9) 8	1	O(9)11	1	2.596	107.2	
	O(9) 9	1	O(9)11	1	2.608	108.3	
SI(9)5	O(8,9)2	1	O(9) 6	1	2.604	107.7	2.623
	O(8,9)2	1	O(9) 9	1	2.631	110.5	
	O(8,9)2	1	O(9)10	1	2.702	114.3	
	O(9) 6	1	O(9) 9	1	2.575	106.6	
	O(9) 6	1	O(9)10	1	2.615	108.3	
	O(9) 9	1	O(9)10	1	2.610	109.1	
SI(9)6	O(10,9)4	1	O(9) 7	2	2.607	108.7	2.624
	O(10,9)4	1	O(9)10	1	2.650	110.6	
	O(10,9)4	1	O(9)12	1	2.602	108.4	
	O(9) 7	2	O(9)10	1	2.606	108.0	
	O(9) 7	2	O(9)12	1	2.678	113.4	
	O(9)10	1	O(9)12	1	2.601	107.7	
SI(9)7	O(8,9)3	1	O(9) 1	6	2.638	109.8	2.627
	O(8,9)3	1	O(9) 4	7	2.609	108.5	
	O(8,9)3	1	O(9)11	1	2.629	110.1	
	O(9) 1	6	O(9) 4	7	2.587	106.6	
	O(9) 1	6	O(9)11	1	2.617	108.7	
	O(9) 4	7	O(9)11	1	2.679	113.2	
SI(9)8	O(8,9)4	1	O(9) 2	6	2.617	109.6	2.623
	O(8,9)4	1	O(9) 3	6	2.618	109.5	
	O(8,9)4	1	O(9)12	1	2.581	107.1	
	O(9) 2	6	O(9) 3	6	2.679	112.8	
	O(9) 2	6	O(9)12	1	2.623	109.2	
	O(9) 3	6	O(9)12	1	2.617	108.5	
SI(10)1	O(10,9)1	1	O(10) 1	1	2.582	106.9	2.620
	O(10,9)1	1	O(10) 2	1	2.598	107.7	
	O(10,9)1	1	O(10) 5	1	2.631	110.0	
	O(10) 1	1	O(10) 2	1	2.620	109.5	
	O(10) 1	1	O(10) 5	1	2.680	113.5	
	O(10) 2	1	O(10) 5	1	2.611	109.1	
SI(10)2	O(10,9)2	1	O(10) 3	1	2.619	109.5	2.618
	O(10,9)2	1	O(10) 4	1	2.564	106.2	
	O(10,9)2	1	O(10) 6	1	2.604	108.4	
	O(10) 3	1	O(10) 4	1	2.643	111.1	
	O(10) 3	1	O(10) 6	1	2.672	112.8	
	O(10) 4	1	O(10) 6	1	2.607	108.6	
SI(10)3	O(10,1)1	1	O(10) 5	1	2.635	110.1	2.625
	O(10,1)1	1	O(10) 7	1	2.607	108.2	
	O(10,1)1	1	O(10) 8	1	2.660	111.9	
	O(10) 5	1	O(10) 7	1	2.587	106.9	
	O(10) 5	1	O(10) 8	1	2.656	111.5	
	O(10) 7	1	O(10) 8	1	2.605	108.1	
SI(10)4	O(10,9)3	1	O(10) 8	1	2.583	107.7	2.617
	O(10,9)3	1	O(10) 9	1	2.671	113.6	
	O(10,9)3	1	O(10)11	1	2.627	110.9	
	O(10) 8	1	O(10) 9	1	2.605	107.9	
	O(10) 8	1	O(10)11	1	2.584	106.7	
	O(10) 9	1	O(10)11	1	2.630	109.9	
SI(10)5	O(10,1)2	1	O(10) 6	1	2.619	109.1	2.627
	O(10,1)2	1	O(10) 9	1	2.595	107.3	
	O(10,1)2	1	O(10)10	1	2.660	111.5	
	O(10) 6	1	O(10) 9	1	2.626	109.4	
	O(10) 6	1	O(10)10	1	2.659	111.0	
	O(10) 9	1	O(10)10	1	2.602	107.8	
SI(10)6	O(10,9)4	1	O(10) 7	2	2.677	113.5	2.621
	O(10,9)4	1	O(10)10	1	2.605	108.2	
	O(10,9)4	1	O(10)12	1	2.624	109.9	
	O(10) 7	2	O(10)10	1	2.598	107.6	
	O(10) 7	2	O(10)12	1	2.644	110.9	
	O(10)10	1	O(10)12	1	2.581	106.4	
SI(10)7	O(10,1)3	1	O(10) 1	6	2.603	108.1	2.617
	O(10,1)3	1	O(10) 4	7	2.562	105.8	
	O(10,1)3	1	O(10)11	1	2.626	109.9	
	O(10) 1	6	O(10) 4	7	2.628	110.1	
	O(10) 1	6	O(10)11	1	2.619	109.8	
	O(10) 4	7	O(10)11	1	2.667	113.0	
SI(10)8	O(10,1)4	1	O(10) 2	6	2.588	107.5	2.621
	O(10,1)4	1	O(10) 3	6	2.611	108.3	
	O(10,1)4	1	O(10)12	1	2.618	109.3	
	O(10) 2	6	O(10) 3	6	2.621	109.4	
	O(10) 2	6	O(10)12	1	2.683	113.9	
	O(10) 3	6	O(10)12	1	2.606	108.4	

main contributors to the weak *uuu* reflections. In fact, the R value is 11% for the 234 7*uu* reflections when the model is composed of only the 80 atoms of the B-type layers. The R for this same subset of *uuu* data is 9% when all 240 atoms are included in the calculation.

There are three other types of pseudosymmetry. Layers 2 and 9 are nearly mirror images of one another across $z = 0{\cdot}25$, as are layers 3 and 8, and layers 4 and 7. The A, C and D layers have approximate screw axes in-plane at $y = 0{\cdot}25$. These are particularly close for layers 3 and 8. The B layers have very approximate centers of symmetry located at the ring centers. The D type of layer differs, after appropriate transformations, by only 0·16–0·20 Å from the C type, so that at some level they may be considered the same.

As shown in Fig. 2, the B layers are sandwiched between layers with approximate $\frac{1}{2}$ cell periodicity. If these layers possessed exact $\frac{1}{2}$ cell periodicity, then

Table 4. Si–Si *distances* (Å) *and* Si–O–Si (°) *angles in low tridymite*

Conventions are as in Table 2. Estimated standard deviation of an individual distance is approximately 0·03 Å.

ATOM 2	ATOM 1	SYM1	ATOM 3	SYM3	DIS	ANG	ATOM 2	ATOM 1	SYM1	ATOM 3	SYM3	DIS	ANG
0(1,2)1	SI(1)1	1	SI(2)1	1	3.156	158.6	0(4) 5	SI(4)1	1	SI(4)3	1	3.065	144.3
0(1,2)2	SI(1)2	1	SI(2)2	1	3.173	173.2	0(4) 6	SI(4)2	1	SI(4)5	1	3.046	141.9
0(1,2)3	SI(1)4	1	SI(2)4	1	3.106	149.6	0(4) 7	SI(4)3	1	SI(4)6	3	3.059	142.7
0(1,2)4	SI(1)6	1	SI(2)6	1	3.092	148.3	0(4) 8	SI(4)3	1	SI(4)4	1	3.094	148.9
0(2,3)1	SI(2)3	1	SI(3)3	1	3.075	145.4	0(4) 9	SI(4)4	1	SI(4)5	1	3.050	141.4
0(2,3)2	SI(2)5	1	SI(3)5	1	3.105	149.6	0(4)10	SI(4)5	1	SI(4)6	1	3.118	151.3
0(2,3)3	SI(2)7	1	SI(3)7	1	3.105	148.8	0(4)11	SI(4)4	1	SI(4)7	1	3.080	146.7
0(2,3)4	SI(2)8	1	SI(3)8	1	3.131	154.7	0(4)12	SI(4)6	1	SI(4)8	1	3.058	144.5
0(3,4)1	SI(3)1	1	SI(4)1	1	3.133	156.5	0(5) 1	SI(5)1	1	SI(5)7	5	3.074	144.8
0(3,4)2	SI(3)2	1	SI(4)2	1	3.082	146.4	0(5) 2	SI(5)1	1	SI(5)8	5	3.056	143.5
0(3,4)3	SI(3)4	1	SI(4)4	1	3.081	146.8	0(5) 3	SI(5)2	1	SI(5)8	5	3.074	145.3
0(3,4)4	SI(3)6	1	SI(4)6	1	3.091	147.1	0(5) 4	SI(5)2	1	SI(5)7	4	3.051	142.7
0(4,5)1	SI(4)3	1	SI(5)3	1	3.105	150.9	0(5) 5	SI(5)1	1	SI(5)3	1	3.146	158.9
0(4,5)2	SI(4)5	1	SI(5)5	1	3.094	148.6	0(5) 6	SI(5)2	1	SI(5)5	1	3.140	158.1
0(4,5)3	SI(4)7	1	SI(5)7	1	3.144	157.6	0(5) 7	SI(5)3	1	SI(5)6	3	3.055	143.1
0(4,5)4	SI(4)8	1	SI(5)8	1	3.148	162.6	0(5) 8	SI(5)3	1	SI(5)4	1	3.108	151.5
0(5,6)1	SI(5)1	1	SI(6)1	1	3.082	147.6	0(5) 9	SI(5)4	1	SI(5)5	1	3.061	143.8
0(5,6)2	SI(5)2	1	SI(6)2	1	3.080	146.8	0(5)10	SI(5)5	1	SI(5)6	1	3.104	151.4
0(5,6)3	SI(5)4	1	SI(6)4	1	3.089	147.2	0(5)11	SI(5)4	1	SI(5)7	1	3.142	158.8
0(5,6)4	SI(5)6	1	SI(6)6	1	3.082	146.5	0(5)12	SI(5)6	1	SI(5)8	1	3.147	158.6
0(6,7)1	SI(6)3	1	SI(7)3	1	3.160	164.7	0(6) 1	SI(6)1	1	SI(6)7	5	3.112	153.0
0(6,7)2	SI(6)5	1	SI(7)5	1	3.161	166.3	0(6) 2	SI(6)1	1	SI(6)8	5	3.067	145.1
0(6,7)3	SI(6)7	1	SI(7)7	1	3.103	149.5	0(6) 3	SI(6)2	1	SI(6)8	5	3.083	147.7
0(6,7)4	SI(6)8	1	SI(7)8	1	3.081	147.0	0(6) 4	SI(6)2	1	SI(6)7	4	3.057	143.1
0(7,8)1	SI(7)1	1	SI(8)1	1	3.108	152.6	0(6) 5	SI(6)1	1	SI(6)3	1	3.125	155.3
0(7,8)2	SI(7)2	1	SI(8)2	1	3.088	147.4	0(6) 6	SI(6)2	1	SI(6)5	1	3.138	157.4
0(7,8)3	SI(7)4	1	SI(8)4	1	3.052	143.1	0(6) 7	SI(6)3	1	SI(6)6	3	3.051	142.5
0(7,8)4	SI(7)6	1	SI(8)6	1	3.073	145.8	0(6) 8	SI(6)3	1	SI(6)4	1	3.051	142.3
0(8,9)1	SI(8)3	1	SI(9)3	1	3.078	145.9	0(6) 9	SI(6)4	1	SI(6)5	1	3.065	142.8
0(8,9)2	SI(8)5	1	SI(9)5	1	3.108	149.1	0(6)10	SI(6)5	1	SI(6)6	1	3.064	144.2
0(8,9)3	SI(8)7	1	SI(9)7	1	3.085	148.0	0(6)11	SI(6)4	1	SI(6)7	1	3.120	151.1
0(8,9)4	SI(8)8	1	SI(9)8	1	3.128	158.1	0(6)12	SI(6)6	1	SI(6)8	1	3.096	149.0
0(10,9)1	SI(9)1	1	SI(10)1	1	3.101	150.0	0(7) 1	SI(7)1	1	SI(7)7	5	3.068	146.0
0(10,9)2	SI(9)2	1	SI(10)2	1	3.085	149.3	0(7) 2	SI(7)1	1	SI(7)8	5	3.066	143.8
0(10,9)3	SI(9)4	1	SI(10)4	1	3.157	167.6	0(7) 3	SI(7)2	1	SI(7)8	5	3.086	147.1
0(10,9)4	SI(9)6	1	SI(10)6	1	3.126	154.7	0(7) 4	SI(7)2	1	SI(7)7	4	3.061	143.5
0(10,1)1	SI(1)5	10	SI(10)3	1	3.104	149.5	0(7) 5	SI(7)1	1	SI(7)3	1	3.086	147.2
0(10,1)2	SI(1)3	8	SI(10)5	1	3.082	146.7	0(7) 6	SI(7)2	1	SI(7)5	1	3.054	142.5
0(10,1)3	SI(1)8	10	SI(10)7	1	3.090	148.0	0(7) 7	SI(7)3	1	SI(7)6	3	3.059	143.3
0(10,1)4	SI(1)7	8	SI(10)8	1	3.091	147.9	0(7) 8	SI(7)3	1	SI(7)4	1	3.089	149.0
0(1) 1	SI(1)1	1	SI(1)7	5	3.061	143.2	0(7) 9	SI(7)4	1	SI(7)5	1	3.026	139.7
0(1) 2	SI(1)1	1	SI(1)8	5	3.051	141.8	0(7)10	SI(7)5	1	SI(7)6	1	3.103	151.6
0(1) 3	SI(1)2	1	SI(1)8	5	3.041	142.2	0(7)11	SI(7)4	1	SI(7)7	1	3.095	148.8
0(1) 4	SI(1)2	1	SI(1)7	4	3.057	142.4	0(7)12	SI(7)6	1	SI(7)8	1	3.067	144.2
0(1) 5	SI(1)1	1	SI(1)3	1	3.167	159.6	0(8) 1	SI(8)1	1	SI(8)7	5	3.066	144.8
0(1) 6	SI(1)2	1	SI(1)5	1	3.152	160.7	0(8) 2	SI(8)1	1	SI(8)8	5	3.070	145.4
0(1) 7	SI(1)3	1	SI(1)6	3	3.094	148.9	0(8) 3	SI(8)2	1	SI(8)8	5	3.064	144.4
0(1) 8	SI(1)3	1	SI(1)4	1	3.056	142.2	0(8) 4	SI(8)2	1	SI(8)7	4	3.065	144.7
0(1) 9	SI(1)4	1	SI(1)5	1	3.089	147.3	0(8) 5	SI(8)1	1	SI(8)3	1	3.104	148.5
0(1)10	SI(1)5	1	SI(1)6	1	3.038	140.4	0(8) 6	SI(8)2	1	SI(8)5	1	3.115	152.1
0(1)11	SI(1)4	1	SI(1)7	1	3.144	157.1	0(8) 7	SI(8)3	1	SI(8)6	3	3.079	146.2
0(1)12	SI(1)6	1	SI(1)8	1	3.136	158.5	0(8) 8	SI(8)3	1	SI(8)4	1	3.089	147.3
0(2) 1	SI(2)1	1	SI(2)7	5	3.055	143.8	0(8) 9	SI(8)4	1	SI(8)5	1	3.089	148.1
0(2) 2	SI(2)1	1	SI(2)8	5	3.092	148.5	0(8)10	SI(8)5	1	SI(8)6	1	3.098	149.7
0(2) 3	SI(2)2	1	SI(2)8	5	3.049	142.3	0(8)11	SI(8)4	1	SI(8)7	1	3.113	151.2
0(2) 4	SI(2)2	1	SI(2)7	4	3.074	146.1	0(8)12	SI(8)6	1	SI(8)8	1	3.127	154.0
0(2) 5	SI(2)1	1	SI(2)3	1	3.081	146.4	0(9) 1	SI(9)1	1	SI(9)7	5	3.063	143.5
0(2) 6	SI(2)2	1	SI(2)5	1	3.056	142.7	0(9) 2	SI(9)1	1	SI(9)8	5	3.087	147.7
0(2) 7	SI(2)3	1	SI(2)6	3	3.094	149.0	0(9) 3	SI(9)2	1	SI(9)8	5	3.042	140.4
0(2) 8	SI(2)3	1	SI(2)4	1	3.061	142.4	0(9) 4	SI(9)2	1	SI(9)7	4	3.099	148.7
0(2) 9	SI(2)4	1	SI(2)5	1	3.142	156.8	0(9) 5	SI(9)1	1	SI(9)3	1	3.093	148.4
0(2)10	SI(2)5	1	SI(2)6	1	3.053	141.9	0(9) 6	SI(9)2	1	SI(9)5	1	3.061	144.1
0(2)11	SI(2)4	1	SI(2)7	1	3.053	142.3	0(9) 7	SI(9)3	1	SI(9)6	3	3.067	146.5
0(2)12	SI(2)6	1	SI(2)8	1	3.076	146.2	0(9) 8	SI(9)3	1	SI(9)4	1	3.042	141.3
0(3) 1	SI(3)1	1	SI(3)7	5	3.051	142.8	0(9) 9	SI(9)4	1	SI(9)5	1	3.087	150.4
0(3) 2	SI(3)1	1	SI(3)8	5	3.060	143.8	0(9)10	SI(9)5	1	SI(9)6	1	3.053	142.1
0(3) 3	SI(3)2	1	SI(3)8	5	3.065	145.0	0(9)11	SI(9)4	1	SI(9)7	1	3.049	142.3
0(3) 4	SI(3)2	1	SI(3)7	4	3.066	145.1	0(9)12	SI(9)6	1	SI(9)8	1	3.064	144.7
0(3) 5	SI(3)1	1	SI(3)3	1	3.119	151.7	0(10) 1	SI(10)1	1	SI(10)7	5	3.060	145.1
0(3) 6	SI(3)2	1	SI(3)5	1	3.119	152.7	0(10) 2	SI(10)1	1	SI(10)8	5	3.106	151.4
0(3) 7	SI(3)3	1	SI(3)6	3	3.092	149.1	0(10) 3	SI(10)2	1	SI(10)8	5	3.061	144.5
0(3) 8	SI(3)3	1	SI(3)4	1	3.094	148.9	0(10) 4	SI(10)2	1	SI(10)7	4	3.094	149.9
0(3) 9	SI(3)4	1	SI(3)5	1	3.080	146.4	0(10) 5	SI(10)1	1	SI(10)3	1	3.105	150.8
0(3)10	SI(3)5	1	SI(3)6	1	3.091	148.7	0(10) 6	SI(10)2	1	SI(10)5	1	3.111	151.2
0(3)11	SI(3)4	1	SI(3)7	1	3.130	155.6	0(10) 7	SI(10)3	1	SI(10)6	3	3.074	145.9
0(3)12	SI(3)6	1	SI(3)8	1	3.106	150.3	0(10) 8	SI(10)3	1	SI(10)4	1	3.061	143.9
0(4) 1	SI(4)1	1	SI(4)7	5	3.093	149.3	0(10) 9	SI(10)4	1	SI(10)5	1	3.070	144.8
0(4) 2	SI(4)1	1	SI(4)8	5	3.041	141.5	0(10)10	SI(10)5	1	SI(10)6	1	3.066	143.7
0(4) 3	SI(4)2	1	SI(4)8	5	3.083	146.7	0(10)11	SI(10)4	1	SI(10)7	1	3.115	153.1
0(4) 4	SI(4)2	1	SI(4)7	4	3.058	143.4	0(10)12	SI(10)6	1	SI(10)8	1	3.125	153.9

shifting the *B* layers by $\frac{1}{2}$ in *x* or *y* (in reality, of course, it would be a series of rotations retaining bonding topology that would have the same result as a shift) would result in exactly the same stereochemistry between the adjacent layers. Evidently, it is because the $\frac{1}{2}$ cell periodicity is not exact that the *B* layers order.

It may be helpful to consider the structure as composed of *ABCBA* layer sequences alternating with *DBCBD* layer sequences. As indicated in Table 6, the *AD,DA* junctions serve approximately as alternating mirror planes and glide planes with respect to the *BCB* sequences. It is worth emphasizing that the two *BCB*

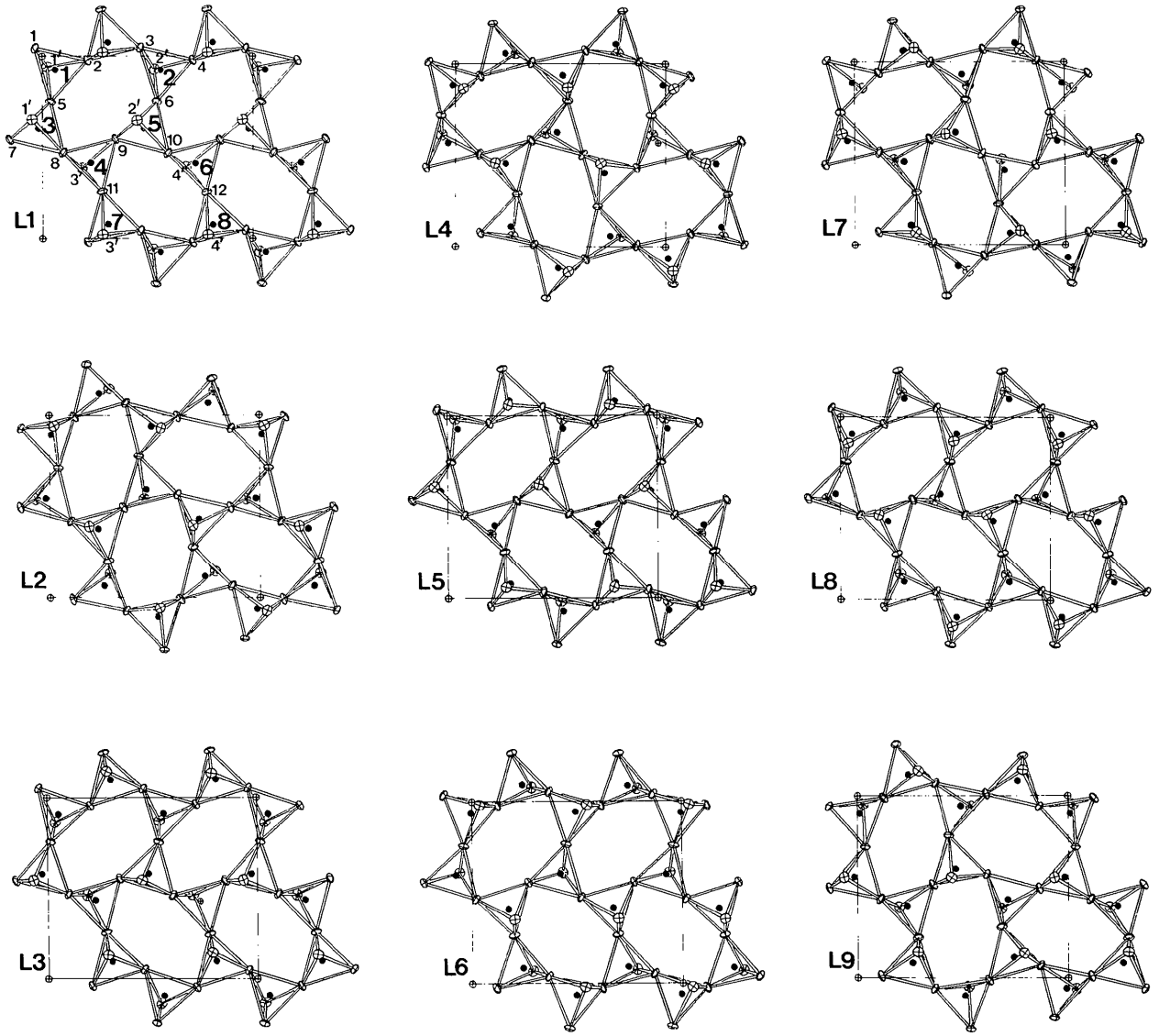

Fig. 1. The structure of low tridymite, shown in layers perpendicular to **c**; **a** across, **b**/2 down. Large numbers (1–8) are Si atoms (dark circles) numbered identically in each layer, corresponding to Tables 1–3. Small unprimed numbers refer to O atoms within the rings which define the layers; small primed numbers refer to O atoms shared with adjacent layers. These also are numbered identically within each layer corresponding to Tables 1–3. The authors have found transparent overlays of the layers useful in viewing the structure.

sequences in the asymmetric unit are only 0·08 Å, on the average, from superimposable; whereas the two *A* layers and the two *D* layers are superimposable to about 0·12 Å. Indeed the 5–6 junction and the 10–1 junction are somewhat different, with the former resulting in an approximate mirror relating the *BCB* sequences and the latter resulting in the near-glide-plane relation.

Models composed of various $\frac{1}{2}$ cell shifts of the *B* layers were used to calculate *R* values for the previously mentioned 7*uu* data subset. The results are summarized in Table 7. Shifting layers 4 and 9 by $\frac{1}{2}a$ resulted in an *R* of 14% *vs* 11% for the refined model.

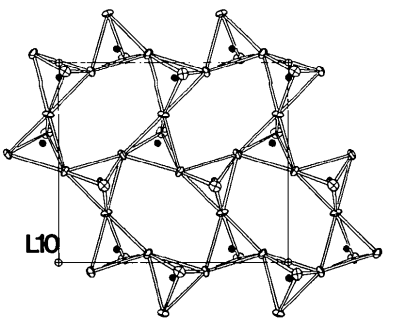

Fig. 1 (*cont.*)

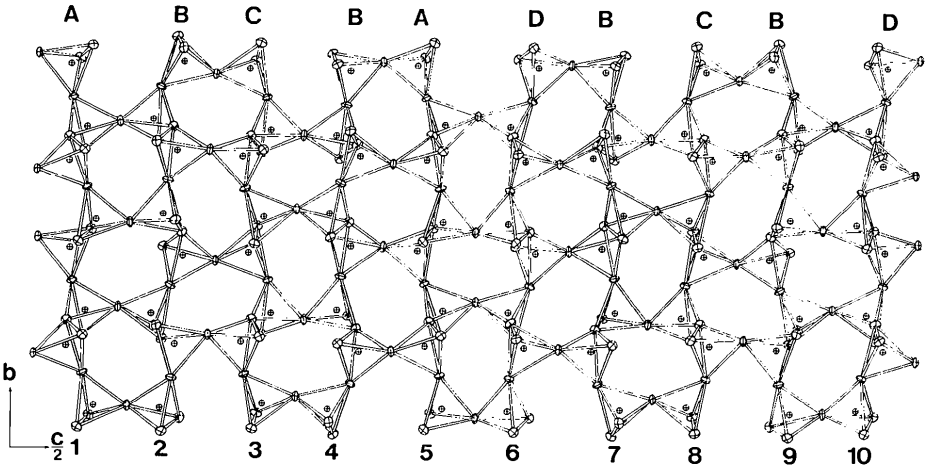

Fig. 2. Sequence of layers in the structure of low tridymite. The layers are numbered as in Fig. 1 and Tables 1–3; letters refer to the layer type as described in the text.

Table 5. *Symmetry transformations used to generate Tables 2–4*

Symmetry number	Translations a	b	c
1	0	0	0
2	1	0	0
3	−1	0	0
4	$\frac{1}{2}$	$-\frac{1}{2}$	0
5	$-\frac{1}{2}$	$-\frac{1}{2}$	0
6	$\frac{1}{2}$	$\frac{1}{2}$	0
7	$-\frac{1}{2}$	$\frac{1}{2}$	0
8	$\frac{1}{2}$	0	$\frac{1}{2}$
9	$\frac{1}{2}$	0	$-\frac{1}{2}$
10	$-\frac{1}{2}$	0	$\frac{1}{2}$
11	$-\frac{1}{2}$	0	$-\frac{1}{2}$

Table 6. *Pseudosymmetric transformations relating layers in low tridymite and average deviations from superimposability for different pairs of layers*

Layer	Type	Approximate transformation			Average deviation from a/2 repeat within the layer
1	*A*	x,	y,	z	0·08 Å
2	*B*	x,	y,	z	0·91
3	*C*	x,	y,	z	0·12
4	*B*	$x-\frac{1}{4}$,	$-y+\frac{1}{2}$,	$-z+\frac{1}{4}$	0·94
5	*A*	$x-\frac{1}{4}$,	$-y+\frac{1}{2}$,	$-z+\frac{1}{4}$	0·08
6	*D*	x,	y,	z	0·10
7	*B*	$x-\frac{1}{4}$,	$-y+\frac{1}{2}$,	$z-\frac{1}{4}$	0·88
8	*C*	x,	y,	$-z+\frac{1}{2}$	0·06
9	*B*	x,	y,	$-z+\frac{1}{2}$	0·90
10	*D*	$x-\frac{1}{4}$,	$-y+\frac{1}{2}$,	$-z+\frac{3}{4}$	0·08

Layers	Average deviation between layers	Type(s)
1–5	0·12 Å	*A*
6–10	0·11	*D*
3–8	0·07	*C*
2–4	0·05	*B*
2–7	0·06	*B*
2–9	0·08	*B*
4–7	0·08	*B*
3–10	0·16	*C–D*
1–3	0·52	*A–C*

These two models represent different levels of refinement of the same structure, and differ only by interchanging the positions of the pseudo-mirrors and pseudo-glides relating the *BCB* sequences. Shifting layers 4 and 7 is similarly the same as shifting 8 and 9. This distinctly different structure refines to an *R* of 8·4%. As summarized in Table 7, various combinations of different structure give remarkably low *R* values. Of all the possibilities, only the 4,9 shift and the 4,7 shift were refined; the former before its relation to the first structure was realized (it refined to the same *R* of 6·4%) and the latter because it possessed the next lowest *R* for the 7*uu* data.

An additional property of the *B* layers is the ability of a chain of tetrahedra in such a layer to change drastically its conformation without altering its linkage with the remainder of the three-dimensional network. In Fig. 3 is depicted layer 9′ at an *R* of 9%. A difference map indicated the true conformation to be that formed by rotations about the darkened tetrahedra edges. When considering transitions and disorders brought on by heating, it may be worth considering such rotations.

Comparison with monoclinic low tridymite

The crystal structure of low tridymite, from material typical of terrestrial occurrences, is reported here. It

Table 7. *Conventional unweighted R values for the 234 7uu reflections for various combinations of B-type layer shifts*

Layers are numbered as in Fig. 2. Only the 80 atoms in *B*-type layers were included.

Layer 2 shift	Layer 4 shift	Layer 7 shift	Layer 9 shift	*R*
0	0	0	0	0·110
0	$\frac{1}{2}$	0	$\frac{1}{2}$	0·139
0	$\frac{1}{2}$	$\frac{1}{2}$	0	0·161
0	0	$\frac{1}{2}$	$\frac{1}{2}$	0·170
0	0	0	$-\frac{1}{2}$	0·202
0	$\frac{1}{2}$	$\frac{1}{2}$	$\frac{1}{2}$	0·212
0	$\frac{1}{2}$	0	0	0·318
0	0	$\frac{1}{2}$	0	0·331

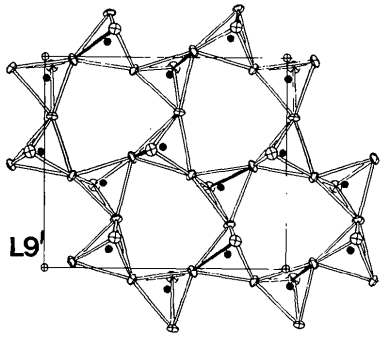

Fig. 3. Layer 9′: an incorrect conformation of layer 9 resulting from rotations about the darkened tetrahedral edges. Labeling conventions are the same as in Fig. 1.

differs significantly from the structure of meteoritic and synthetic 'low-tridymites' as described by Dollase & Baur (1976) and Kato & Nukui (1976). Gardner & Appleman (1974) pointed out that even the corresponding orthorhombic subcells of these two types of tridymite show a volume difference of approximately 4·1%. The terrestrial tridymite which we studied has ten crystallographically distinct layers, and the six-membered rings of tetrahedra which form these layers are all 'oval' (Fig. 1). In contrast, meteoritic tridymite has only two crystallographically distinct layers, and these layers contain $\frac{1}{3}$ 'oval' and $\frac{2}{3}$ 'ditrigonal' rings (Dollase & Baur, 1976). The reasons for the much greater complexity of the terrestrial material remain unclear. Some pertinent comparisons with the structure of Dollase & Baur follow.

The interatomic distances and angles in the two structures are similar. Average Si–O distances for individual tetrahedra range from 1·602 to 1·611 Å (terrestrial) and from 1·587 to 1·616 Å (meteoritic), but the significance of the differences is not certain, in view of the constraints applied in our refinement. Si–Si nearest-neighbor distances range from 3·03 to 3·17 Å (terrestrial, Table 4), and from 3·04 to 3·18 Å (meteoritic). The Si–O–Si angles correspondingly range from 139·7 to 173·2° with an average of 148·3° (terrestrial) and from 141·7 to 178·5° with an average of 149·8° (meteoritic). In both structures, there is only one very large Si–O–Si angle. Only five of the Si–O–Si angles are greater than 160° in the terrestrial structure. All of these large Si–O–Si angles are between layers rather than within a layer. The average Si–O–Si angles found in these structures are close to those observed in other SiO_2 polymorphs (O'Keeffe & Hyde, 1976).

The average isotropic temperature factors are significantly higher in the meteoritic structure than in the terrestrial tridymite: B_{av}(Si) = 0·61 (terrestrial), 0·93 (meteoritic); B_{av}(O) = 1·48 (terrestrial), 1·93 Å^2 (meteoritic). It seems possible that the meteoritic and synthetic compounds represent a higher-temperature form of tridymite with more positional disorder. It is noteworthy that, as pointed out by Dollase & Baur (1976), individual cristobalite- and tridymite-like structures generally have only one type of ring configuration: either all oval or all ditrigonal. Low cristobalite has all oval rings, high cristobalite may have all ditrigonal rings. By tenuous analogy, meteoritic 'low-tridymite', with $\frac{1}{3}$ oval and $\frac{2}{3}$ ditrigonal rings, may represent a higher-temperature modification than terrestrial low tridymite, with all oval rings.

No evidence was found for ordering of aluminum into particular tetrahedral sites. Indeed, the chemical analysis shows slightly less than one of the 80 tetrahedral atoms to be aluminum. At the current level of refinement, we are unable to detect any ordering of atoms within the structural cavities. Our results fail to show any effects of impurities in stabilizing the tridymite structure.

The authors wish to thank Stephen P. Gardner, the Fenn School, for selecting and photographing the crystal used in this study, while a student at Princeton University. Dr Jerome Karle and Dr Wayne A. Hendrickson, Naval Research Laboratory, provided helpful discussions. Eugene Jarosewich, Smithsonian Institution, aided in the chemical analysis.

References

Appleman, D. E., Nissen, H.-U., Stewart, D. B., Clark, J. R., Dowty, E. & Huebner, J. S. (1971). *Proc. 2nd Lunar Sci. Conf.* **1**, 117–113.

Baur, W. H. (1977). *Acta Cryst.* B**33**, 2615–2619.

Dollase, W. A. (1967). *Acta Cryst.* **23**, 617–623.

Dollase, W. A. & Baur, W. H. (1976). *Am. Mineral.* **61**, 971–978.

Dollase, W. A., Cliff, R. A. & Wetherill, G. W. (1971). *Proc. 2nd Lunar Sci. Conf.* **1**, 141–142.

Gardner, S. P. & Appleman, D. E. (1974). *Am. Crystallogr. Assoc. Program Abstr. Ser.* 2, **2**, 271.

HESTENES, M. R. & STIEFEL, E. (1952). *J. Res. Natl Bur. Stand.* **49**, 409–436.
KARLE, J. & KARLE, I. L. (1966). *Acta Cryst.* **21**, 849–859.
KATO, V. K. & NUKUI, A. (1976). *Acta Cryst.* B**32**, 2486–2491.
KONNERT, J. H. (1976). *Acta Cryst.* A**32**, 614–617.
KONNERT, J. H. & APPLEMAN, D. E. (1975). *Geol. Soc. Am. Abstr. Programs*, **7**, 1151.
KONNERT, J. H. & KARLE, J. (1972). *Nature (London) Phys. Sci.* **236**, 92–94.
O'KEEFFE, M. & HYDE, B. G. (1976). *Acta Cryst.* B**33**, 2923–2936.
RATH, G. VOM (1868). *Ann. Phys. (Leipzig)*, **135**, 437.
STEWART, J. M., KRUGER, G. J., AMMON, H. L., DICKINSON, C. & HALL, S. R. (1972). XRAY system – version of June 1972. Tech. Rep. TR-192. Computer Science Center, Univ. of Maryland, College Park, Maryland.
WASER, J. (1963). *Acta Cryst.* **16**, 1091–1094.
ZACHARIASEN, W. H. (1967). *Acta Cryst.* **23**, 558–564.

Acta Cryst. (1978). B**34**, 403–406

Structure Cristalline du Polysulfure de Lanthane LaS_2

PAR JÉRÔME DUGUÉ, DANIEL CARRÉ ET MICHELINE GUITTARD

Laboratoire de Physique et Laboratoire de Chimie Minérale Structurale (Laboratoire associé au CNRS n°200), Faculté des Sciences Pharmaceutiques et Biologiques de l'Université René Descartes, 4 avenue de l'Observatoire, 75270 Paris CEDEX 06, France

(*Reçu le* 17 *juin* 1977, *accepté le* 13 *septembre* 1977)

Lanthanum disulphide, LaS_2, is orthorhombic, space group *Pnma*, with unit-cell constants $a = 8{\cdot}131$ (5), $b = 16{\cdot}34$ (1), $c = 4{\cdot}142$ (2) Å and $Z = 8$. The crystal structure has been determined from Syntex automatic diffractometer data, using Patterson and Fourier syntheses, and refined by the least-squares method to a final R of 0·045. Sheets of (LaS), parallel to the [100] axis, are formed from La_5S pyramids; between these layers, planes of S atoms are inserted, formed from S–S pairs in which the interatomic distance (2·104 Å) indicates a covalent bond. The structure is related to a distorted arrangement of anti-Fe_2As type.

Introduction

De nombreux travaux ont déjà été réalisés sur les polysulfures des terres rares LnS_2, mais l'accord ne s'est pas encore fait sur leur maille cristalline.

Flahaut, Guittard & Patrie (1959) ont décrit, il y a longtemps, d'après des diagrammes de Debye et Scherrer, les polysulfures LnS_2 (Ln = La, Ce, Pr, Nd et Sm) comme ayant une maille cristalline de symétrie cubique. Marcon & Pascard (1968) indiquent que le polysulfure de cérium CeS_2 est isotype du polysélénure $CeSe_2$, de symétrie monoclinique; mais leur détermination de la structure du polysélénieure $CeSe_2$, effectuée sur monocristal, n'a pu les conduire qu'à une valeur du R des cristallographes égale à 0,14.

Yanagisawa & Kume (1973) préparent, sous haute pression, un polysulfure de cérium dont la maille cristalline présente une symétrie orthorhombique, et donnent pour constantes du réseau: $a = 8{,}11$; $b = 16{,}20$; $c = 4{,}09$ Å. Mais ils n'ont ni déterminé le groupe spatial, ni résolu la structure.

Seule a été déterminée par une étude sur monocristal, jusqu'à une valeur finale de R égale à 0,042, la structure d'un polysulfure d'ytterbium YbS_2 (Teske, 1974); cette phase, différente du composé que nous avons étudié, possède une maille cristalline de symétrie monoclinique, dont les constantes sont: $a = 9{,}32_6$; $b = 4{,}75_4$; $c = 9{,}02_5$ Å; $\beta = 118{,}3_9°$.

Préparation

Nous préparons le polysulfure de lanthane LaS_2 par chauffage, à 700 °C en ampoule de silice vide d'air, d'un mélange de sesquisulfure de lanthane La_2S_3 et de soufre en quantité stoechiométrique.

La poudre cristalline ainsi obtenue, mélangée à cinq parties de l'eutectique KI–KCl, est chauffée, toujours en ampoule de silice, à 750 °C pendant trois semaines, puis refroidie lentement. Après lavage à l'eau froide, on recueille de nombreux cristaux transparents, de couleur rouge orangé, ayant la forme de plaquettes. A partir de